

**GEOLOGY OF PART OF THE AREA EAST AND WEST OF
QUEBRADAS ROAD BETWEEN MILE MARKERS 15
AND 20, SOCORRO COUNTY, NEW MEXICO**

By

Frank Marshall Craig

Submitted in partial fulfillment of the requirements
for the degree of Master of Science
in Geology

New Mexico Institute of Mining and Technology

Socorro, New Mexico

September, 1992

In memory of my grandfather, Frank Craig, who passed
away shortly after my arrival in New Mexico.

ABSTRACT

The study area is located on the east side of the Rio Grande rift within the southeastern portion of the Socorro Accommodation Zone. The area has been subjected to, at least, Laramide and Rio Grande rift related deformation. This superposition of differing tectonic styles has resulted in a structurally complex area. In general, the area contains broad, faulted folds; faults are low- and high-angle. locally, folds may be tightly compressed or overturned. Rocks involved in the deformation range in age from Pennsylvanian to upper Triassic. Units include the upper Pennsylvanian Madera Formation; the Permian Bursum, Abo, Yeso, Glorieta, and San Andres Formations; and the upper Triassic Santa Rosa and San Pedro Arroyo Formations.

Low-angle faults and folds are the oldest structures in the study area. Low-angle faults formed first, followed by, or occurring simultaneously with, the formation of broad, gentle folds. Local, tight asymmetric to overturned mesoscopic folds have been interpreted as fault-propagation folds or drag folds related to low-angle faulting. The age of the deformation can be constrained to post-upper Triassic, pre-upper Cretaceous.

The low-angle faults and folds are offset by northeast- and northwest-striking high-angle faults. Movement along most of the northwest-striking faults can be attributed to a left-lateral wrench system which developed in response to an approximately N70W directed compression. Movement along one of the northwest-striking faults was right-lateral, suggesting a rotation of the maximum principal stress to approximately N08E. The age of this deformation, except for the right-lateral motion, can be constrained to the upper Cretaceous.

Rift related high-angle faults and reactivation of low-angle faults as gravity slides are the youngest structures in the study area. A north-striking fault on the west side of the study area is a late rift, en echelon fault system. The age of reactivation cannot be determined accurately. Because rift faults are currently active, it is possible for reactivation and rifting to be occurring simultaneously.

Small-scale, tightly compressed or overturned folds may be related to an uppermost Permian or early Triassic deformation event. This type of folding and related low-angle faulting appears to be confined to upper Pennsylvanian and lower Permian strata, however, it cannot be distinguished from upper Cretaceous deformation. Therefore, the earliest deformation is considered to be the Laramide orogeny. Chapin and Cather (1981) have proposed a two stage Laramide orogeny for New Mexico. The oldest deformation in the study area fits the early stage of their model. Northwest-striking faults do not fit their model suggesting more than two stages of Laramide deformation.

ACKNOWLEDGMENTS

I would like to thank my advisor, Clay T. Smith, who first introduced me to the area and its numerous structural complexities. Many discussions and field excursions helped immensely in the identification of stratigraphic units and providing an understanding of the structural development of the area. Thanks are also extended to committee members Peter Mozley and Paul Bauer for their helpful comments on various aspects of this study. Discussions with many other people have also improved the quality of this study. In particular, I wish to thank Chris Beck, Jacques Renault and Gus Armstrong (USGS) of the New Mexico Bureau of Mines and Mineral Resources, and Bob Colpitts who helped in the interpretations of structures observed in the field. I would like to thank Gus Armstrong for identification of fossils and the identification and interpretation of carbonate lithologies.

I am indebted to the New Mexico Bureau of Mines and Mineral Resources (C. E. Chapin, Director) for the generous loan of a field vehicle and to Ed Fry who acted as a chauffeur when a Bureau vehicle was not available.

I would also like to acknowledge the NMT Geoscience Department for the loan of a Brunton compass and Pam Pinson for the use of her compass while the department's was at field camp. Part of field expenditures were covered by a grant from the "Antonius and Anita Budding Graduate Research Fund".

Last, but certainly not least, I would like to thank my parents, Frank and Jean Craig, without whose moral and financial support this study would not have been possible.

Table of Contents

Abstract	i
Acknowledgements	ii
Table of Contents	iii
List of Figures	vi
List of Tables	x
INTRODUCTION	1
Location and Accessibility	1
Previous Work	1
Purpose	3
Methods	4
STRATIGRAPHY	5
Introduction	5
Pennsylvanian System	5
Madera Formation	5
Permian System	9
Bursum Formation	11
Abo Formation	12
Yeso Formation	14
Meseta Blanca Member	16
Torres Member	17
Cañas Gypsum Member	18
Joyita Sandstone Member	19
Glorieta Formation	20
San Andres Formation	21
Triassic System	23
Santa Rosa Formation	24
San Pedro Arroyo Formation	25
Tertiary System	26
Santa Fe Group	26
Tertiary Dikes	26
Quaternary System	27
STRUCTURAL GEOLOGY	28
Introduction	28
Folds	31
Mesoscopic Folds	33
Fold A	33
Fold B	33
Fold C	36
Fold D	36

Drag Folds	36
Macroscopic Folds	41
Fold II	41
Fold III	41
Fold IV	44
Fold V	44
Faults	46
North- and Northeast-striking Faults	46
Fault 1	48
Fault 2	48
Fault 3	48
Fault 4	49
Fault 5	49
Fault 6	52
Northwest-striking Faults	52
Fault 7	52
Fault 8	53
Faults 9 - 13	56
Fault 14	56
Fault 15	57
Fault 16	57
Low-Angle Faults	58
Older beds over younger	60
Younger beds over older	63
Eastern Ridge	64
Southeastern Ridges	70
Silica Crystallite Geothermometry	71
Other Structures	75
STRUCTURAL ANALYSIS	75
Mesoscopic Fold Analysis	75
Fold A	75
Fold B	78
Fold C	78
Macroscopic Fold Analysis	78
Origin of Folds	79
Fold A	82
Fold B	85
Fold C	89
Fold D	89
High-angle Fault Analysis	92
Fault 1	92
Fault 2	92
Fault 3	92

Fault 4	93
Fault 5	93
Fault 6	93
Fault 7	93
Fault 8	94
Faults 9-13	94
Fault 14-15	94
Fault 16	94
Origin of Faults	95
Northeast-striking Faults	95
Northwest-striking Faults	95
North-striking Faults	96
Low-angle Fault Analysis	96
Older beds over younger	96
Younger beds over older	98
Geothermometry Analysis	98
 STRUCTURAL HISTORY	 101
Episode 1	101
Episode 2	102
Episode 3	104
Regional Implications	105
 REFERENCES	 107

List of Figures

Figure 1. Map showing the location of the present field area as well as previous thesis areas (modified after BLM, 1991).	2
Figure 2. Upper Paleozoic and Mesozoic stratigraphic column for the Socorro region (modified after Osburn and Lochman-Balk, 1983)	7
Figure 3. Photograph of solution planes in the Madera Formation; NW1/4, NW1/4, Sec. 17. Hammer for scale is approximately 25 cm long. . . .	10
Figure 4. Photograph of a limestone pebble conglomerate within the Abo Formation showing interbedded nature; SW1/4, Sec. 16. Lens cap for scale.	15
Figure 5. Photograph of salt casts commonly found within the Meseta Blanca Member of the Yeso Formation.	17
Figure 6. Location of the study area with respect to regional structures. Base map after Christiansen and Kottlowski (1972). Structure after deVoogd (1986), Hawley (1978), Yuras (1976), and Chapin (1971).	29
Figure 7. Map of the study area illustrating the locations of structural features.	32
Figure 8. View to the southeast of Fold A at the base of the duplex in figure 21 (p. 61). V. Herne for scale is approximately 1.5 m tall.	34
Figure 9. View to the north of asymmetric folding in Meseta Blanca beds. V. Herne for scale is approximately 1.5 m tall.	35
Figure 10. View to the northwest of folds within Meseta Blanca beds overturned to the southwest. V. Herne for scale is approximately 1.5 m tall. SW1/4, SW1/4, Sec. 5.	37
Figure 11. Sketch of composite photograph of imbricate system in the SW1/4, SW1/4, Sec. 5. Also shown is Fold D.	38
Figure 12a. View to the northwest of fold train in footwall of a thrust; SW1/4, SW1/4, Sec. 5. Folds are developed in incompetent beds of the Torres Member. Pen for scale is 15 cm long.	39

Figure 12b. View to the Northwest of a single drag fold in the footwall of a small ramp; SW1/4, SW1/4, Sec. 5. Fold developed in competent bed of Meseta Blanca Member. Pen for scale is 15 cm long.	40
Figure 13. View to the north of ridge in eastern part of area showing synclinal structure.	42
Figure 14. View to the northeast of the nose of an anticline plunging to the north; NE1/4, NW1/4, Sec. 16. Fold developed in Torres Member of the Yeso Formation.	43
Figure 15. View to the southwest of asymmetric fold in the Abo Formation; NE1/4, SW1/4, Sec. 16. C. Beck for scale is approximately 2 m tall.	45
Figure 16. Contoured stereonet plot (Lambert equal-area net, lower hemisphere projection) of faults within the field area.	47
Figure 17. View to the north of gouge zone of Fault 4 cutting low-angle fault between San Andres and Glorieta Formations. S = San Andres Formation; B = Breccia; and G = Gouge. Hammer for scale is 34 cm long.	50
Figure 18. Photograph of fault zone (Fault 4) SE1/4, NW1/4, SW1/4, Sec. 9 showing breccia (B) and travertine (T). Pen for scale is 15 cm long and oriented 355°.	51
Figure 19a. Scatter diagram (Lambert equal-area net, lower hemisphere projection) of slickenside striae orientations in Area 1 showing type of motion. Great circle represents orientation of Fault 7.	54
Figure 19b. Contoured (1% area) plot (Lambert equal-area net, lower hemisphere projection) of data in figure 19a showing three areas of concentration (labelled I through III). Great circle represents orientation of bedding in Area 1.	55
Figure 20. View to the northwest of breccia zone (left half) related to movement along Fault 16. Right half of the photo is Meseta Blanca Member of the Yeso Formation. Dog for scale is .6 m tall.	59
Figure 21. View to the southeast of duplex at the east end of the arroyo, west of Quebradas Road; SW1/4 SW1/4 Sec. 5. V. Herne for scale is approximately 1.5 m tall.	61

Figure 22. View to the south of small ramp-flat geometry in the Meseta Blanca Member of the Yeso Formation; SW1/4, SW1/4, Sec. 5. Isaac for scale is approximately 1.7 m tall.	62
Figure 23. View to the northwest of low-angle fault surfaces of the east side of the ridge. S = San Andres Formation; G = Glorieta Formation; J = Joyita Member, Yeso Formation; C = Cañas Member, Yeso Formation; and T = Torres Member, Yeso Formation.	66
Figure 24. View to the southwest of a Type I breccia showing clasts of the Glorieta (G) and San Andres (S) Formations. Hammer for scale is 34 cm long.	67
Figure 25. View to the northwest of a Type II breccia NW1/4, NE1/4, Sec. 16. Knife for scale is 28 cm long.	68
Figure 26. View to the northwest of low-angle fault in the San Andres Formation, NW1/4, NE1/4, Sec. 16. Dead tree, bottom right, is approximately 1.5 m tall.	72
Figure 27. The mosaic structure of a real crystal (after Cullity, 1978).	74
Figure 28. View to the southwest of mesoscopic folds in the Madera Formation, Sec. 17.	76
Figure 29. View to the northwest of low-angle faulting in the Madera Formation, Sec. 17. C. Smith for scale is approximately 1.7 m tall.	77
Figure 30. Three types of fold-thrust interactions: (a) a fault-bend fold, (b) a fault propagation fold, and (c) a detachment fold (after Jamison, 1987).	81
Figure 31. Balanced structural models showing (a) synclinal breakthrough structure and (b) anticlinal breakthrough structure (after Suppe and Medwedeff, 1990)	83
Figure 32. a) Schematic drawing of a general angular parallel fault-propagation fold. b) Relationship between fault shape, θ , and fold shape γ and γ^* for constant thickness fault-propagation folding with lines of constant cutoff angle θ_1 (after Suppe and Medwedeff, 1991).	84

- Figure 33. Sketch of fold in figure 8 using the kink method of reconstruction. The colored layer represents the bed that was traced from the photograph (marker horizon); the fold shape was reconstructed based on the marker horizon. 86
- Figure 34. Influence of shear in fold core layers in simple-step fault-propagation folds with constant ramp height. Shear decreases from (a) through (d); step up angle for all four cases is 30°. Fold core angles, γ^* , are: (a) 25°, (b) 30°, (c) 40°, and (d) 50° (after Mosar and Suppe, 1992). 87
- Figure 35a. Trace of marker horizon in figure 9 (dashed) and reconstructed using the kink method (solid). 88
- Figure 35b. Reconstructed fault-propagation fold based on data obtained from the marker horizon (colored) in figure 35a. Solid lines represent units exposed above the surface. Dashed lines represent what the beds would look like in subsurface and if Fault 7 did not offset the fold. F represents the approximate location of where Fault 7 will cut the fold. 90
- Figure 36. Possible interpretation of the tight fold in figure 9. Solid lines represent beds observed in outcrop. Dotted lines represent beds covered in outcrop. Dashed lines in subsurface represent structure in subsurface suggested by surface outcrops. 91
- Figure 37. Restoration of duplex in figure 21 by line length balancing. Dashed lines represent locations of faults after restoration. 97
- Figure 38. Schematic sketch of a thrust sheet demonstrating the placement of younger strata over older strata. 99
- Plate 1. Geologic map of part of the area east and west of Quebradas Road between mile markers 15 and 20, Socorro County, New Mexico. Back Pocket
- Plate 2. Cross Sections A-A' to J-J'. Back Pocket

List of Tables

Table 1. Strike and dip of thrust faults measured from east to west in arroyo in
SW1/4,SW1/4, Sec. 5. 63

Table 2. Summary of deformation within the study area. 101

INTRODUCTION

Location and Accessibility

The study area is located 12 km (8 mi) due northeast of San Antonio, New Mexico in central Socorro County (Fig. 1). The field area covers approximately 7 sq. mi and includes sections 5, 8, 17, and parts of 6, 7, and 18, T.4 S., R.2 E. and the S1/4 of sections 31 and 32, T.3 S., R.2 E. in the San Antonio Quadrangle as well as parts of sections 4, 9, and 16 T.4 S., R.2 E. in the Cañon Agua Bueno Quadrangle. Quebradas road (BLM maintained dirt road recently named a Back Country By-Way), which runs south from Pueblito, New Mexico to Socorro County Rt. A-129, approximately bisects the field area, providing easy access, weather permitting.

Previous Work

The earliest geologic studies in the region were by Lee (1909) who prepared a stratigraphic section of the Abo and Yeso Formations, and by Darton (1922, 1928) who prepared a geologic map and cross sections approximately 20 km (13 mi) north of the present study area. Wilpolt and Wanek (1951) published a reconnaissance map, cross sections, and stratigraphic sections of a portion of central Socorro County to aid in the exploration for oil, gas, and economic minerals.

Most of the work after Wilpolt and Wanek (1951) was done as thesis studies by students at the New Mexico Institute of Mining and Technology. This includes detailed mapping and stratigraphic work by Rejas (1965), Maulsby (1981), Bauch (1982) and Smith et. al. (1991) to the north, and Fagrelus (1982) to the south. Seimers (1978)

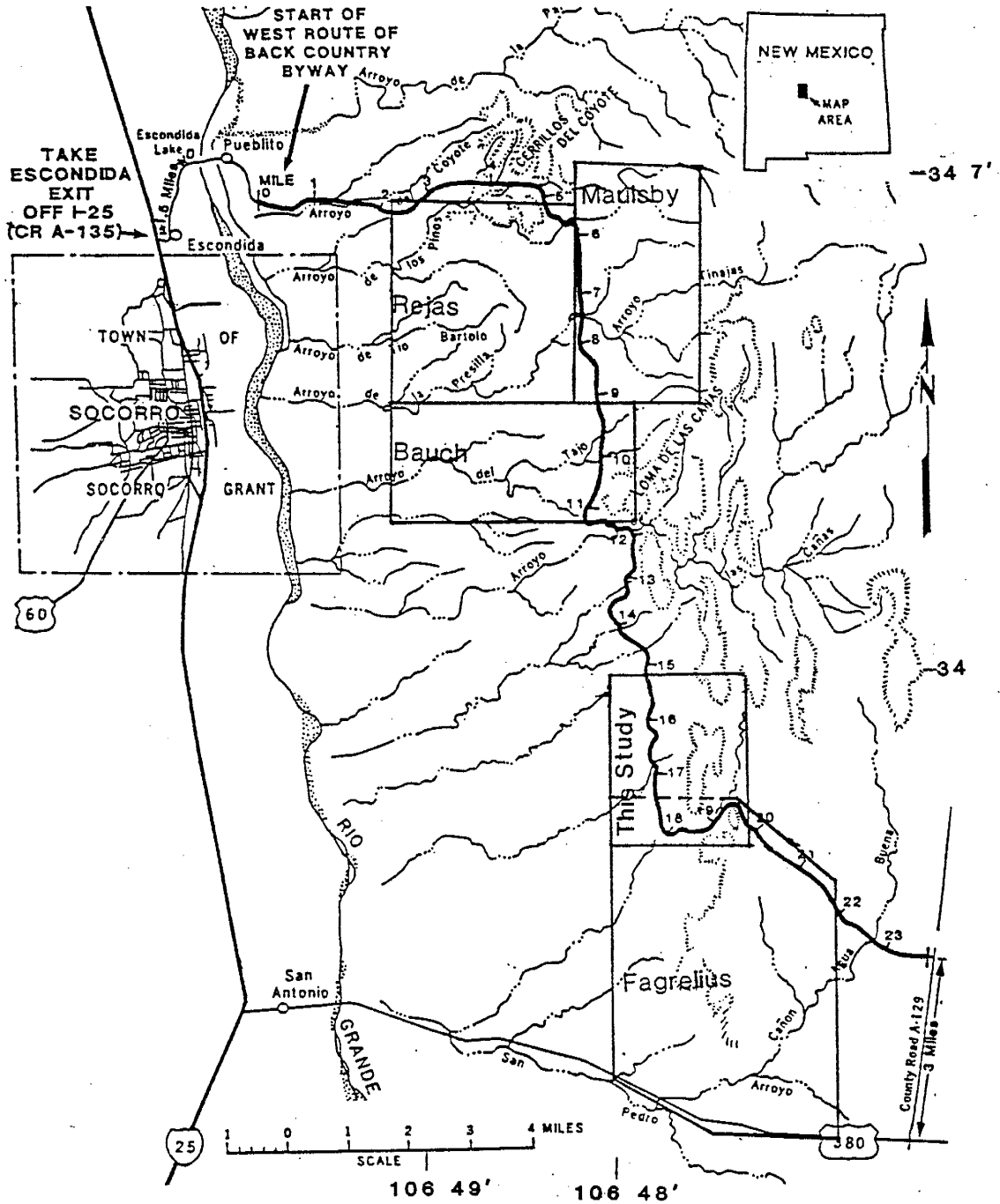


Figure 1. Map showing the location of the present field area as well as previous thesis areas (modified after BLM, 1991).

completed a comprehensive stratigraphic and petrologic study of the Pennsylvanian system in the Socorro Region, but did not include a detailed map. Smith et. al. (1983) prepared a road log for a New Mexico Geological Society Field Conference which included one stop within the present study area.

Other studies pertinent to this research include Colpitts (1986), Brown (1987), and Linden (1990). These authors worked in the Mesa del Yeso Area, approximately 20 km (13 mi) north of the study area.

Purpose

Previous studies indicate that part of the area east and west of Quebradas Road between mile markers 15 and 20 has experienced at least two episodes of tectonism: shortening associated with the Laramide orogeny, and extension associated with the development of the Rio Grande rift. Evidence for a third period of late Permian or early Triassic deformation is suggested by data from Rejas (1965), Maulsby (1981), Bauch (1982), Fagrelus (1982), and C.T. Smith (pers. com., 1990),. The existence of an analogous (?) deformational event during the interval Permian---Jurassic has been documented by Stone and Stevens (1990) in southeastern California (and possibly Nevada), by Tosdal (1990) in southeastern California and southwestern Arizona and by Walker et. al. (1990) in the Mojave desert, California.

This study has two main objectives. First, the resulting map and structural-stratigraphic data will fill part of the gap which now exists between the northern map areas of Rejas (1965), Maulsby (1982), Bauch (1982), and Smith et. al. (1991), and the

southern map area of Fagrelius (1982). Second, the structural history of the area will help to constrain regional tectonic synthesis, and may aid in evaluating the possibility of a Permo-Triassic deformational event in central New Mexico.

Methods

Data collection involved detailed mapping of the various stratigraphic units, orientation measurements of faults, folds, slickenside lineation, etc. and time distribution of various geologic formations. Mapping was carried out on enlarged portions of (scale 1:12,000) USGS 7.5 minute topographic sheets supplemented by areal photographs. Structural analyses involved equal-area stereographic projection of fault planes, folds, etc.. Orientation diagrams were prepared using the computer program "Fabric" (Starkey, 1970, 1978). Stratigraphic analysis primarily involved field descriptions; only a few thin-sections were cut.

STRATIGRAPHY

INTRODUCTION

Rocks ranging in age from Pennsylvanian to Quaternary are well exposed within the study area. Units include the Pennsylvanian Madera Limestone; the Permian Bursum, Abo, Yeso, Glorieta, San Andres, and Artesia Formations; the Triassic San Pedro Arroyo and Santa Rosa Formations; the Tertiary Santa Fe Group (undifferentiated); and Quaternary alluvial deposits. Regional dips, gentle folding, and block faulting cause the Pennsylvanian and Permian strata to young towards the east. Tertiary and Quaternary units bound the region to the east and west. Triassic beds occur in the extreme southeastern corner of the area and are in fault contact with strata of Permian age.

PENNSYLVANIAN SYSTEM

Madera Formation

The name Madera was proposed by Keyes (1903) for the massive upper Pennsylvanian blue-gray limestones exposed in the cliffs of the Sandia Mountains (most likely named after the town of La Madera; Thompson, 1944). In subsequent papers Keyes (1905, 1906) used the term Madera with reference to limestones not belonging to the upper Pennsylvanian. Because Keyes did not place a strict definition on the term it was also used in different senses by later investigators as well (Thompson, 1942). This led Thompson (1942) to propose that the term Madera be excluded from Pennsylvanian nomenclature. In its place, Thompson was able to divide the Madera into four groups

and ten formations based on the presence of fusulinids. However, these subdivisions are not well constrained lithologically, and Bates et. al. (1947) proposed that the term Madera be retained to include all lithologies above the Sandia Formation and below the Bursum Formation where detailed faunal studies are not feasible. Based on lithology, the Madera Limestone can be divided into a lower limestone unit (gray limestone member) and an upper mixed limestone-clastic unit (arkosic limestone member) (Siemers, 1978). Because of the nature of the exposures within the field area this nomenclature is used in this study (Fig. 2).

Gordon (1907) first proposed the name Magdalena as a group term to include all lithologies between the Kelly Limestone (Mississippian) and the Abo Formation (Permian) in the Magdalena Mountains and other areas. Although this rank term was accepted by the U.S. Geological Survey, the New Mexico Bureau of Mines and Mineral Resources no longer uses the term (Bates et. al. 1947). The main reason for the term being abandoned is a redundancy in stratigraphic nomenclature. Thompson (1942) stated that the "term Magdalena seems to be essentially synonymous with the systematic term Pennsylvanian." King (1945) had stated, in an objection to the Hueco Formation being included in the Magdalena Group, "the names Pennsylvanian and Hueco are fully adequate for designation of those strata, and it is recommended that the term Magdalena, a relic of an antiquated type of stratigraphic nomenclature, be permanently abandoned." However, the transitional nature of the Bursum Formation into Wolfcampian makes the group usage reasonable (Fig. 2)

In the Socorro region the Madera varies in thickness from 64 to 716 m (210 -

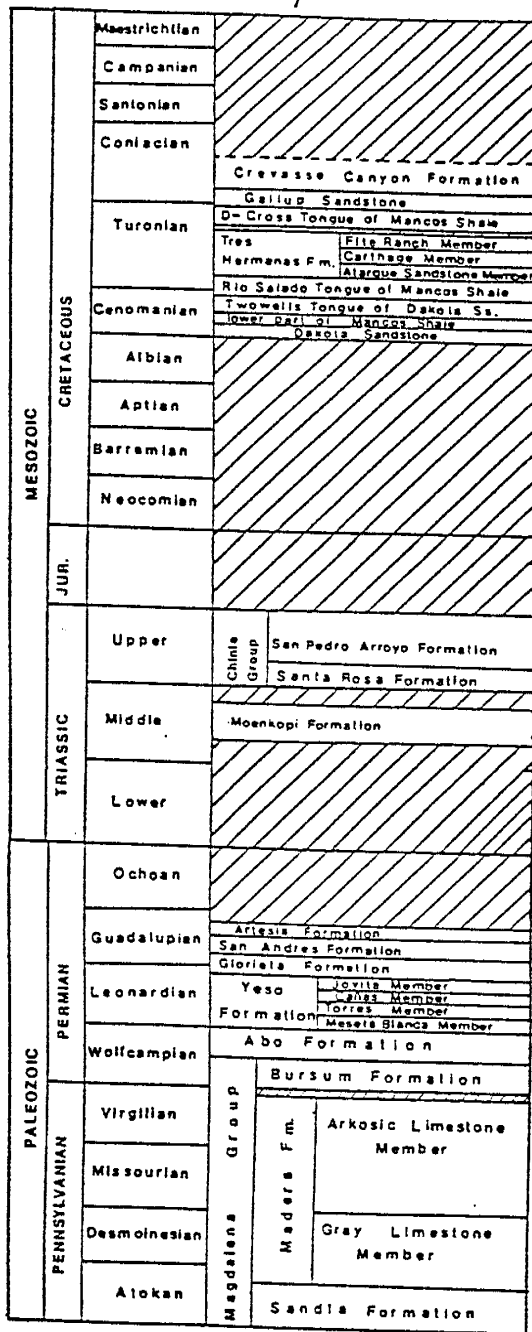


Figure 2. Upper Paleozoic and Mesozoic stratigraphic column for the Socorro region (modified after Osburn and Lochman-Balk, 1983)

2349 ft), with the thickest sections occurring in the southern Ladron, Magdalena, and southeastern San Mateo Mountains (Siemers, 1983). Fagrelus (1982) measured an incomplete thickness of 58.5 m (192 ft) in the Cerro del Viboro area, part of which is included in the southwestern part of the map area of this study.

Within the field area the Madera Formation crops out as a single uplifted block in the SE 1/4, Sec. 7, W 1/4 Sec. 17 and the E 1/4 Sec. 18, T.4 S., R.2 E. of the San Antonio Quadrangle. It is bounded by high angle faults on the north and west and offset by numerous northwest-striking faults. It consists of a thick-bedded, cherty limestone interbedded with shales overlying a thick sequence of clastic sediments interbedded with minor limestone units (Arkosic Limestone Member; Osburn and Lochman-Balk, 1983). The contact with arkoses of the overlying Bursum Formation on the east appears conformable.

The clastic sequence crops out as three distinct units on the west slope of the block. These units are separated by covered sections which are most likely shale (based on outcrops in the arroyo bottom and minimal exposures observed on the slope). The lowermost unit is a poorly sorted, light gray arkose. The next unit is a .9 m (3 ft) thick laminated light gray siltstone (cm thick laminae). The uppermost unit is 1.8 m (6 ft) thick, moderately-well sorted, light gray, fine-grained arkose. It is interbedded with laminated siltstones 1 to 2 cm thick. Sedimentary structures present include trough cross-bedding, convolute bedding, and graded bedding. Grain size varies from .5 mm to 4mm.

The overlying limestone forms a cycle of two limestones and two slopes (composed of shale, in part, with the rest of the section covered), with a slope unit

cropping out at the base of the cycle. The limestone units are 3 to 4.6 m (10 -15 ft) in thickness interbedded with slope forming units 4.6 to 6.1 m (15 - 20 ft) in thickness. On top of this cycle is a thin, 1 m (3.25 ft) thick, pale green, fossiliferous micrite consisting of bryozoans, brachiopods, and crinoid columnals; a few rugosan corals were found but these are relatively rare. The brachiopod shells are disarticulated and randomly oriented indicating a death assemblage. The top of the Madera Formation consists of a massive light gray to gray micrite approximately 9 m (30 ft) thick. The only sedimentary structures present within this unit are planes which resemble bedding but are most likely related to dissolution (i.e stylolites). These solution planes predominate in the lower part of the unit where they form sequences .9 m (3 ft) in thickness (Fig. 3). All of the limestone beds have been pervasively replaced by chert in the form of nodules and lenses. Nodular chert tends to weather to a dark brown, whereas lenses or pods of chert weather to a tan color.

PERMIAN SYSTEM

Permian strata are exposed as incomplete sequences consisting of a maximum of 596 m (measured to the south by Fagrelus, 1982) of sandstones, shales, siltstones, and gypsum. Measurement in most sections is complicated by folding, faulting, and minor cover.

Bursum Formation

The Bursum Formation was first described by Wilpolt et. al. (1946) from a

described in the report of the U.S. Geol. Surv., T. 28 N., R. 4 E., Missouri County, near the
Dunlap road, with the name and address of the U.S. Geol. Surv. office, and the
type section name (Madera) by T. C. M. A., 1907, in the U.S. Geol. Surv., T. 28 N., R. 4



Figure 3. Photograph of solution planes in the Madera Formation; NW1/4, NW1/4, Sec. 17.

Hammer for scale is approximately 25 cm long.

designated type section in the SE 1/4 Sec. 1, T.6 S., R.4 E., Socorro County, near the Bursum triangulation station (Jicha and Lochman-Balk, 1958). Sections other than the type section were measured by Bates et. al. (1947) in the NE 1/4 Sec. 14, T.2 N., R.4 E., Socorro County, and 5.4 km (3.5 mi) to the northeast in Abo Canyon; by Colpitts (1986) from the SE 1/4, NW 1/4, Sec. 12, T.2 S., R.2 E. to the E 1/2, Sec. 12, T.2 S., R.2 E., Cañoncito de la Uva; and by Altares (1990) who measured five complete sections in central Socorro County.

At the type locality the Bursum consists of 76 m (249 ft) of thick sequences of dark purplish red and green shales separated by thinner beds of arkosic conglomerate and gray limestone (Wilpolt et. al., 1946). Altares (1990) measured a 41 m (135 ft) section within the field area (W1/4 Sec. 17, T.4 S., R.2 E.) which consists of interbedded carbonate mudstones, arkosic sandstone, and claystone.

Within the field area the Bursum is exposed along the western margin of the map in W 1/4 Sec. 17, W 1/4 Sec. 8, NE 1/4 Sec. 7 and E 1/2 Sec. 6, T.4 S., R.2 E. and consists of a dark purple, poorly-sorted, matrix-supported arkose interbedded with limestone. The quartz grains are angular to subrounded and most of the feldspar grains are angular. Grain size varies from approximately .5 mm to 3 mm. Within this "dirty" arkose occur lenses of "clean" arkose composed of 20 to 25 % feldspar and 75 to 80% quartz. The limestones are usually less than 10 ft thick and consist of fossiliferous micrite. Fossils include fusulinids and mollusc fragments (probably gastropods). The limestone is locally nodular.

Abo Formation

The Abo Formation derives its name from 'Abo Canyon', the drainage which separates the southern Manzano Mountains from the Los Pinos Mountains. Lee (1909) first described the formation as 152 to 243 m (499 - 797 ft) of dark red to purple coarse-grained sandstone with a basal conglomerate and subordinate amounts of shale. The formation was redescribed by Needham and Bates (1943) because Lee did not designate a specific type locality. Lee also underestimated the percentage of shale and included limestone units either of Pennsylvanian age or belonging within the Bursum Formation. The type section, located near the village of Scholle in Abo Canyon, consists of 247 m (810 ft) of red shale (62.8 %); red to pink, fine- to medium-grained, locally cross-bedded sandstones (36.6 %); and conglomerate (0.6 %) conformably overlying limestone of the Bursum Formation (Needham and Bates, 1943). Red beds of the Abo Formation exposed within the Puertocito Quadrangle, located in northwestern Socorro County, have been divided into two members based on lithology by Tonking (1957). The lower member consists of 213 m (699 ft) of interbedded dark-grayish-red to reddish brown siltstone, shale, arkose and lenses of limestone-pellet conglomerate. The upper member consists of 61 m (200 ft) of grayish yellow to light-reddish-brown, thin- to medium-bedded, very fine- to fine-grained feldspathic sandstones and siltstones.

The paleontology of the Abo Formation was first considered by Girty (1909) in conjunction with the study of the Manzano Group carried out by Lee (1909). Girty identified a diverse fauna of brachiopods, cnidarians, bryozoans and bivalves. Unfortunately, the fossils identified were collected by Lee (1909) from limestone units

now considered to be part of the underlying Madera Formation (Pennsylvanian; see Fig. 2). The Abo does contain casts of gymnosperm (conifer) fragments which were first reported by White (1933). Recent work by Hunt (1983) placed the occurrence of the fossil flora mainly within the upper member of the formation. In addition, trace fossils (dominantly burrows) are commonly associated with the plant casts.

The age of the Abo Formation, and the Manzano Group in general, was determined by Lee (1909) to be upper Pennsylvanian based on the correlation of invertebrate fossils known to be Pennsylvanian in age from the midwestern and eastern United States. Lee did not observe any plant fossils within the red beds of the Abo Formation. White (1933) concluded from paleobotanical evidence and Darton (1922) from invertebrate fossil evidence that the Abo was Permian in age. Based on plant biostratigraphy, Hunt (1983) concluded that the Abo Formation varies in age vertically and possibly laterally from Wolfcampian to Leonardian (see Fig. 2). Plant fossils assigned to the genera *Callipteris*, *Gigantopteris* and *Supaia* have the potential for being Permian index fossils; however, more work needs to be done and additional localities found (Hunt, 1983).

The Abo Formation is exposed along the western margin of the map area in sec. 17, Sec. 8 and the W1/4 Sec. 5, and as a fault-bounded block in the E1/4 Sec. 17 and SW1/4 Sec. 16. It consists of interbedded sandstones, siltstones and mudstones. The Abo Formation tends to form gentle hills and dip-slope cuestas where resistant sand and siltstone ledges protect less resistant mudstones. The thickness of the Abo was calculated to be 236 m (773 ft) based on outcrop pattern. Sedimentary structures include cross-

bedding, desiccation cracks, ripple marks, and reduction spots. Trace fossils and casts of conifer fragments are present, but are not common.

In the southern part of the field area (SW1/4 Sec. 16, T.4 S., R.2 E.) the sandstones are interbedded with a limestone-pebble conglomerate (Fig. 4). These conglomerate beds range from 5 cm to 61 cm in thickness; the thicker beds were deposited in small channels. Limestone fragments vary in size from < 1 mm to approximately 5 mm and occasionally show fining upward sequences. The grains are angular to subrounded and are matrix supported which indicates a source area close by. The presence of these conglomerates suggests that during deposition of the Abo Formation there were remanent Pennsylvanian highlands that periodically shed material into the basin (W.C. Beck, pers. com., 1992).

Yeso Formation

Lee (1909) first proposed the name 'Yeso' for the 305 to 610 m (1000 - 2000 ft) of sandstones, shales, limestones and gypsum exposed at Mesa del Yeso located 8 km northeast of Socorro. The stratigraphic section measured was located 1.2 km south of the mesa. The Yeso was redescribed by Needham and Bates (1943) because the section measured by Lee was faulted and contained units of the Glorieta sandstone and San Andres Limestone. The section measured by Needham and Bates is located 3 km northeast of Socorro and consisted of 181 m (594 ft) of sandstone, siltstone, shale, limestone and gypsum. This section is also faulted and incomplete and a thickness of 299 m (987 ft) measured at Sierra de la Cruz, 4.6 to 6.2 km (3 to 4 mi) east of Mesa del



Figure 4. Photograph of a limestone pebble conglomerate within the Abo Formation showing interbedded nature; SW1.4, Sec. 16. Lens cap for scale.

Yeso by Colpitts (1986) is considered to be a complete section. To the northwest in the Zuni Mountains and to the southeast in the Oscura Mountains the Yeso Formation is approximately 380 m (1246 ft) thick (C.T. Smith, pers. com., 1992).

The Yeso Formation can be subdivided into four members (first suggested by Needham and Bates, 1943). These are: the Meseta Blanca member (basal unit), the Torres member, the Cañas Gypsum member and the Joyita sandstone member. The basal member was named by Wood and Northrop (1946) for a succession of siltstones and sandstones originally assigned to the upper Abo Formation by Needham and Bates (1943). The Torres member, named by Wilpolt et. al. (1946), consists of interbedded sandstone, siltstone, limestone, and, in some locations, gypsum. The Cañas dominantly consists of white to gray gypsum interbedded with red to pink gypsiferous sandstone (Bates et. al., 1947). The Joyita consists of pink to gray sandstone and siltstone. The thickness of individual members varies between localities.

Meseta Blanca Member

The Meseta Blanca member is exposed in the northwestern part of the map area in the W1/2 Sec. 8 and the W1/4 Sec. 5. and in the southern part of the area in the E1/2 Sec. 17. This unit is predominantly composed of sandstone and siltstone with minor amounts of mudstone (usually less than a foot when present). Sedimentary structures include ripple marks and salt casts (Fig. 5).

The Meseta Blanca Member can be distinguished from the Abo Formation by the following characteristics: (1) the color of the Meseta Blanca is typically lighter than the

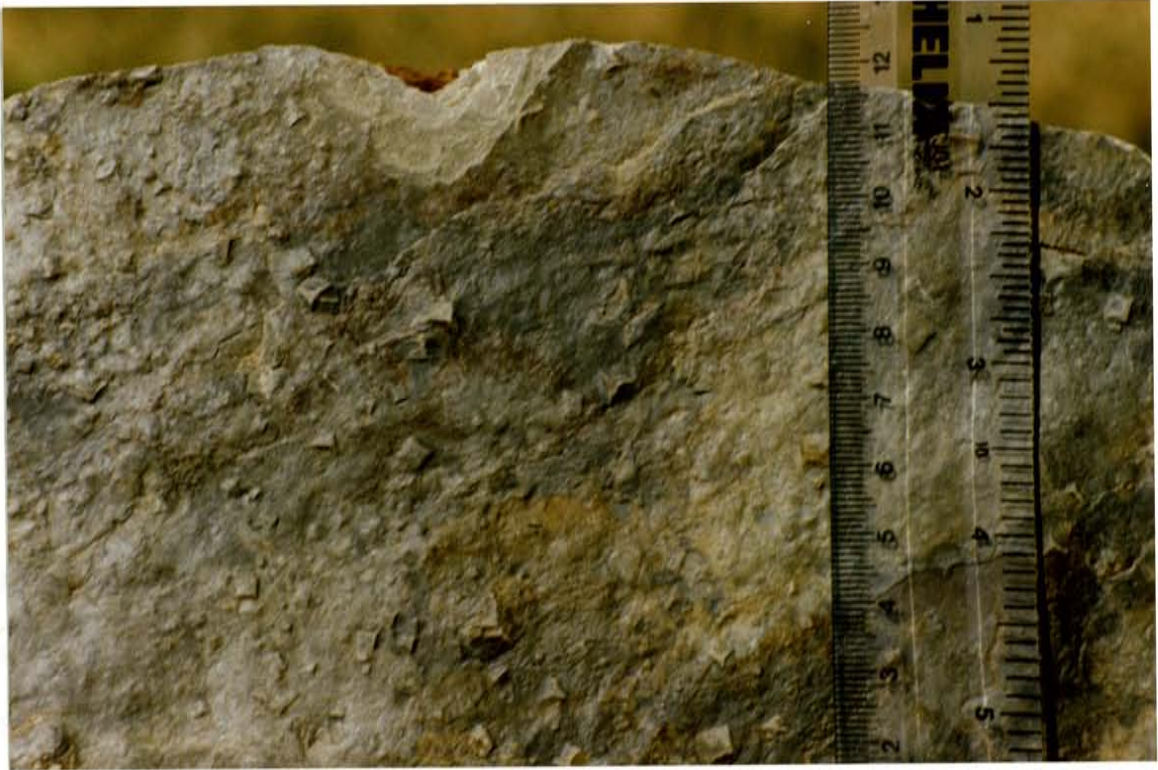


Figure 5. Photograph of salt casts within the Meseta Blanca Member of the Yeso Formation. Scale is in cm

Abo, (2) the Meseta Blanca commonly contains abundant salt casts, (3) the Meseta Blanca has a lower shale/sandstone ratio (W.C. Beck, pers. com., 1990), and (4) the Meseta Blanca is usually better sorted (C.T. Smith, pers. com., 1992).

For mapping purposes, the contact with the Torres Member can be placed at the base of the first limestone unit. Stratigraphically, the contact is placed at a change in grain size between siltstones of the Meseta Blanca Member (usually pink) and the coarser siltstones and sandstones beneath the first limestone of the Torres Member (usually yellow).

Torres Member

The Torres Member is distributed throughout the area northeast of Fault 8. Between the two major northwest-striking faults (Fault 8 and Fault 16; Plate 1) the member forms an arcuate outcrop pattern around the high-standing block in the E1/2, Sec. 8 (hereafter referred to as the 'eastern ridge'). The Torres Member consists of interbedded sandstones, siltstones, gypsum, and limestone. The gypsum tends to form a minor part of the cycle in the lower part of the section, becoming more important towards the top where it can be as thick as 6.1 to 9.1 m (20 -30 ft) with no siltstone.

The limestones are light gray, gray-brown, or light tan micrites and are approximately 5 feet thick. Most of the limestones are structureless, but some contain laminations. The clastic sequences show local sedimentary structures. The gypsum is sometimes bedded but mostly occurs as lenses or pods. Fossils within the limestone units are rare, usually confined to the lowermost and uppermost units. Fossils which occur

in the first limestone consist of echinoid spines (A.K. Armstrong, pers. com., 1991) and small brachiopods.

The contact with the overlying Cañas Member is a low-angle fault and is mapped at the top of the last limestone unit in the area; no carbonate is present above this limestone.

Cañas Gypsum Member

The Cañas Gypsum Member crops out around the base of the eastern ridge and forms poorly exposed pods and lens shaped outcrops. The gypsum is white to gray and is very-fine grained. It usually contains folded, black laminations. Layers not showing laminations contain crystals of selenite embedded in a white fine-grained matrix. The gypsum weathers to a blocky appearance with fine-grained gypsum occurring between raised ridges of selenite fracture fill.

The contact between the Cañas and Joyita members is placed at the lithologic break between gypsum and siltstone; this contact is also a low-angle fault.

Joyita Sandstone Member

The Joyita Sandstone Member is moderately well exposed around the eastern ridge and consists of 0 to 31 m (0 to 100 ft) of sandstone. The sandstone is light brick-red to pinkish-red and consists of moderately-well to well-sorted, rounded to well-rounded quartz grains; trace amounts of potassium feldspar were noted. It is friable and commonly contains veins of calcite and/or gypsum where it is in contact with limestones

of the Torres Member and/or gypsum of the Cañas Member.

The contact with the overlying Glorieta Formation is a low-angle fault and was placed at the change in color from red to white as well as a change in grain size from finer to coarser.

Glorieta Formation

The term Glorieta was first used by Keyes (1915, in Jicha and Lochman-Balk, 1958, p. 53) who applied it to rocks subsequently correlated with the Cretaceous Dakota Formation in the Southern Rocky Mountains. Keyes most likely named the sandstone (no type section was designated) from either Glorieta Mesa or the town of Glorieta, which is situated on Glorieta mesa, even though no outcrops of Cretaceous strata occur on the Mesa (Needham and Bates, 1943). The Glorieta was first designated as Permian in age by Hagar and Robitaille (1919, in Jicha and Lochman-Balk, 1958, p.53) who placed it in the upper Yeso Formation as a member. After about 1940, literature of the U.S. Geological Survey ranked the Glorieta sandstone as the lower member of the San Andres Formation (Jicha and Lochman-Balk, 1958). The first detailed description of the Glorieta was made by Needham and Bates (1943) who designated a type section "... in Glorieta Mesa 0.65 km (1 mi) west of the village of Rowe, San Miguel County, New Mexico." The measured section consisted of 42 m (136 ft) of what now would be called a medium- to coarse-grained buff to white gray quartz arenite. Needham and Bates (1943) also promoted the sandstone to the rank of formation because of "its wide distribution, persistence of lithology, bold topographic expression, and stratigraphic

importance." In many areas of New Mexico, the New Mexico Bureau of Mines and Mineral Resources recognizes the Glorieta as a separate formation. However, the unit thins to the south of Socorro and Kottowski et. al. (1956) and King (1945) report that when the Glorieta is present it is practically indistinguishable from the underlying Yeso Formation. Because the Glorieta is a distinctive and mappable unit in the study area it is treated as a separate formation.

The Glorieta Formation is one of the cliff forming units of the long ridge in the east half of Sec. 8 and also crops out on the smaller ridges in the southeast corner of the map. It is approximately 40 - 75 m (150 - 250 ft) in thickness consisting of individual beds as much as 2 m (6 ft) thick. It is composed of medium-grained, well-rounded, and well-sorted, frosted quartz grains. It is off white on fresh surface but weathers to a light gray. Beds are slightly fissile and show spheroidal weathering. Sedimentary structures include trough cross-bedding.

The contact with the overlying San Andres Formation is a low-angle fault characterized by a breccia zone of variable thickness.

San Andres Formation

The San Andres Formation derives its name from the San Andres (formerly San Andreas) Mountains, south-central New Mexico, where Lee (1909) designated a type section at the northern end of the range (now known as Rhodes Canyon). At this locality Lee measured a section consisting of massive, chert bearing limestones (named the San Andreas Limestone) that are approximately 152 m (499 ft) thick. Darton (1928) changed

the spelling to San Andres Limestone and ranks it as a member in his Chupadera Formation (named from Chupadera Mesa in eastern Socorro County). He describes the lithology as consisting of limestone and gray sandstone. The gray sandstone mentioned is the Glorieta sandstone. Darton measured a 244 m (800 ft) section of the Chupadera Formation near Rhodes Canyon; however, he included the Yeso Formation as a member of his Chupadera Formation. Needham and Bates (1943) returned to Rhodes Canyon and measured a section in more detail and defined a specific type locality. They reported 181 m (594 ft) of predominantly limestone with some dolomitic beds; at Chupadera Mesa a 5 m (16 ft) thick sandstone unit was found to occur 6 m (20 ft) above the base of the formation (Needham and Bates, 1943). Kottlowski et. al. (1956) remeasured the Rhodes Canyon section and measured two additional sections in the San Andres Mountains. The formation was found to thin southward from 183 m (600 ft) at Rhodes Canyon to 117 m (384 ft) in the southern San Andres Mountains (Kottlowski et. al., 1956). They also collected a "varied molluscan fauna" from the upper beds in Rhodes Canyon indicative of Leonardian age. The San Andres Formation has been correlated with the Kaibab Limestone of Arizona and the Colorado Plateau based on lithologic, faunal and stratigraphic similarities (see Baars, 1962).

The San Andres Formation caps both of the major ridges in the eastern part of the map area. It contains an incomplete section due to erosion and faulting of interbedded micritic units and grainstones. The micrites are light gray and form beds that range in thickness from .9 to 1.8 m (3 to 6 ft). The grainstones are dark gray and are usually about .9 m (3 ft) thick. Fossils occur at certain horizons within the micrite

and include mollusc fragments (probably gastropods) and abundant brachiopods. Molds of nautiloid Cephalopods replaced with dolomite (A.K. Armstrong, pers. com., 1992) occur within a black layer approximately .5 m (1.5 ft) thick (this layer is probably a lens).

TRIASSIC SYSTEM

Upper Triassic and lower Cretaceous strata occur in the extreme southeastern part of the study area; these units extend south to the Carthage area (Fagrelius, 1982). Outcrops are scattered and a combined thickness of 582 m of sandstones, siltstones, and shales was measured by Fagrelius (1982).

In the past, Upper Triassic strata exposed in the region have been referred to as 'Dockum Group' or 'Dockum Formation' (Wilpolt and Wanek, 1951; Kottowski et. al., 1956; Kottowski, 1963; Fagrelius, 1982; and Colpitts, 1986). Triassic nomenclature has recently undergone a radical revision due to the extensive studies of Triassic strata east of the Rio Grande (Lucas and Hayden, 1989; Lucas and Hunt, 1989; Lucas, 1991a; Lucas, 1991b; Lucas and Anderson, 1992). The Middle Triassic Moenkopi Formation is now believed to extend across the Rio Grande into the Carthage area (O.J. Anderson, pers. com., 1992). The Santa Rosa Formation (previously called the Santa Rosa Sandstone; Darton, 1922; Fagrelius, 1982) has been retained and includes early Upper Triassic strata. The mud dominated section above the Santa Rosa was previously referred to as Chinle Formation (Fagrelius, 1982). The Chinle has been raised to a group rank term which includes all Upper Triassic strata (see Lucas, 1991b). The name

San Pedro Arroyo Formation has been proposed by Lucas (1991b) for the mudstone dominated strata of the Chinle Group in south-central New Mexico. The San Pedro Arroyo Formation correlates with the Garita Creek and Trujillo Formations and possibly the Lower Bull Canyon Formation in east-central New Mexico (Lucas and Anderson, 1992).

The revised Upper Triassic nomenclature is used in this study (see Fig. 2 pg. 7).

Santa Rosa Formation

The Santa Rosa Formation crops out in the southeastern corner of the study area and is in fault contact (Fault 1) with the Glorieta and San Andres Formations. Most of the formation is covered by alluvium but near Fault 1 it consists of interbedded fine sandstone and coarse arkose. The sandstones are light gray and are predominantly quartz with a minor amount of biotite (< 10%). Quartz grains are angular to subrounded and are moderately sorted. Sandstone beds are approximately 1 m (3.5 ft) thick and are laminated. Arkose is brownish-gray and consists of poorly sorted angular feldspar grains (25%) and rounded to subrounded quartz grains cemented with hematitic matrix. Arkose layers are approximately .8 m (2.5 ft) thick and display planar cross beds.

San Pedro Arroyo Formation

The San Pedro Arroyo Formation was first named and described by Lucas (1991b). The type section is located in San Pedro Arroyo, which is a tributary of the Rio Grande that parallels NM-380 on the north, "in the northern fourth of T.5 S., R.2

E., Socorro County" (Lucas, 1991b). Here the formation is approximately 123 m (403 ft) thick and consists of variegated mudstones (67%) interbedded with sandstone, conglomerate, and siltstones. In Socorro and Valencia Counties a limestone interval occurs in the lower part of the formation. This limestone has been named the Ojo Huelos Member by Lucas (1991b).

The San Pedro Arroyo Formation crops out in the extreme southeastern corner of the study area. It consists of interbedded mudstone, sandstone, and siltstone with the mudstone making up approximately 70% of the section. The sandstones are grayish-green, brownish-red, or light gray and consist of approximately 60% quartz, 30% biotite, and 10% lithics. The light gray sandstones are predominantly quartz with no mica. Quartz grains are subangular to subrounded and are poorly to moderately sorted. The siltstones are reddish-brown, poorly sorted, and consist primarily of subangular quartz grains with minor mica. The siltstones and sandstones are less than .6 m (2 ft) thick and commonly thickly laminated. The mudstones are variegated purple, green, red, and maroon and range in thickness from .6 m (2 ft) to 15.24 m (50 ft) or more.

TERTIARY SYSTEM

Santa Fe Group

The Santa Fe Group crops out along the western margin of the study area where it is either offset by or covers the eastern faults of the rift. It is reddish-brown to light tan and consists mainly of a matrix supported cobble and boulder conglomerate. The matrix is a very-coarse grained lithic arkose. The quartz grains are subangular to

subrounded and make up approximately 50% of the rock. The feldspar grains are angular and make up approximately 24%. Lithic fragments make up the remaining 26%. Conglomerate clasts range in size from 2.54 to 31 cm and show a crude imbrication toward the west. The composition of the clasts ranges from siltstone\sandstone to limestone and the beds are derived from erosion of local formations. For example, brick red siltstones are probably derived from the Abo Formation; arkoses may come from the Bursum or Madera Formations; sandstone and limestone are usually Glorieta or San Andres clasts. The average exposed thickness of the group in the study area is approximately 15 m (50 ft).

Tertiary Dikes

An andesite dike crops out in the SW1/4, SW1/4, Sec. 9, T.4 S., R.2 E. The dike is approximately 6 m (20 ft) wide and approximately 92 m (300 ft) long. The dike is irregularly exposed and occurs as patchy outcrops within the Torres Member. It weathers green brown and contains vugs due to preferential weathering of the phenocrysts. The andesite is green to black on fresh surface with phenocrysts of altered plagioclase and hornblende.

QUATERNARY SYSTEM

Recent alluvial deposits occur as stream alluvium, dune deposits, and talus deposits. Stream alluvial deposits are tan, brown, and red and consist of poorly sorted, unconsolidated sand to boulder sized clasts. The composition of the clasts varies

depending on the formation bordering the arroyo. Talus deposits occur on the slopes of all the hills in the study area and consist of unconsolidated gravel to boulders derived from the erosion of the hills. Dune deposits occur in two areas: the NW1/4, NW1/4, Sec. 8, T.4 S., R.2 E. and the NW1/4, SE1/4, Sec. 7, T.4 S., R.2 E.. They are tan to yellow and consist of fine, well-sorted quartz grains.

STRUCTURAL GEOLOGY

INTRODUCTION

The study area is located on the east side of the Rio Grande rift within the southeastern portion of the Socorro Accommodation Zone (Chapin, 1978, 1989; Fig. 6) - a narrow zone separating the wider expressions of the rift, the Albuquerque-Belen Basin to the north and the San Marcial and Jornada del Muerto Basins to the south and southeast. These basins are part of a series of en echelon north-trending grabens or half grabens that form the Rio Grande depression, a late Cenozoic extensional feature that extends from Leadville, Colorado to Sonora, Mexico (Chapin, 1971). The depression has been superimposed on a structural trend consisting of Laramide and Ancestral Rocky Mountain deformation (Beck and Chapin, 1991) and a Precambrian structural fabric defined by gravity and aeromagnetic data (Cordell, 1978). The Precambrian structural fabric is known to have been influential in Laramide and Ancestral Rocky Mountain deformation and is suspected to have been influential in rift development (Beck, 1991). Some Laramide structures are believed to have been reactivated during rift extension (Kelly, 1977; deVoogd et. al., 1986; Cather and Chapin, 1989). This superposition of deformation has resulted in a structurally complex area. In general, the study area contains broad folds, gently plunging to the north, which have been faulted. Locally, folds may be tightly compressed and overturned. Faults are both high- and low-angle.

Within the region of the study area high-angle faults, with dips in excess of 60°, can be divided into three groups based on orientation (Smith, 1983): (1) N-striking; (2) NE-striking; and (3) NW-striking. Rejas (1965) originally recognized the first two

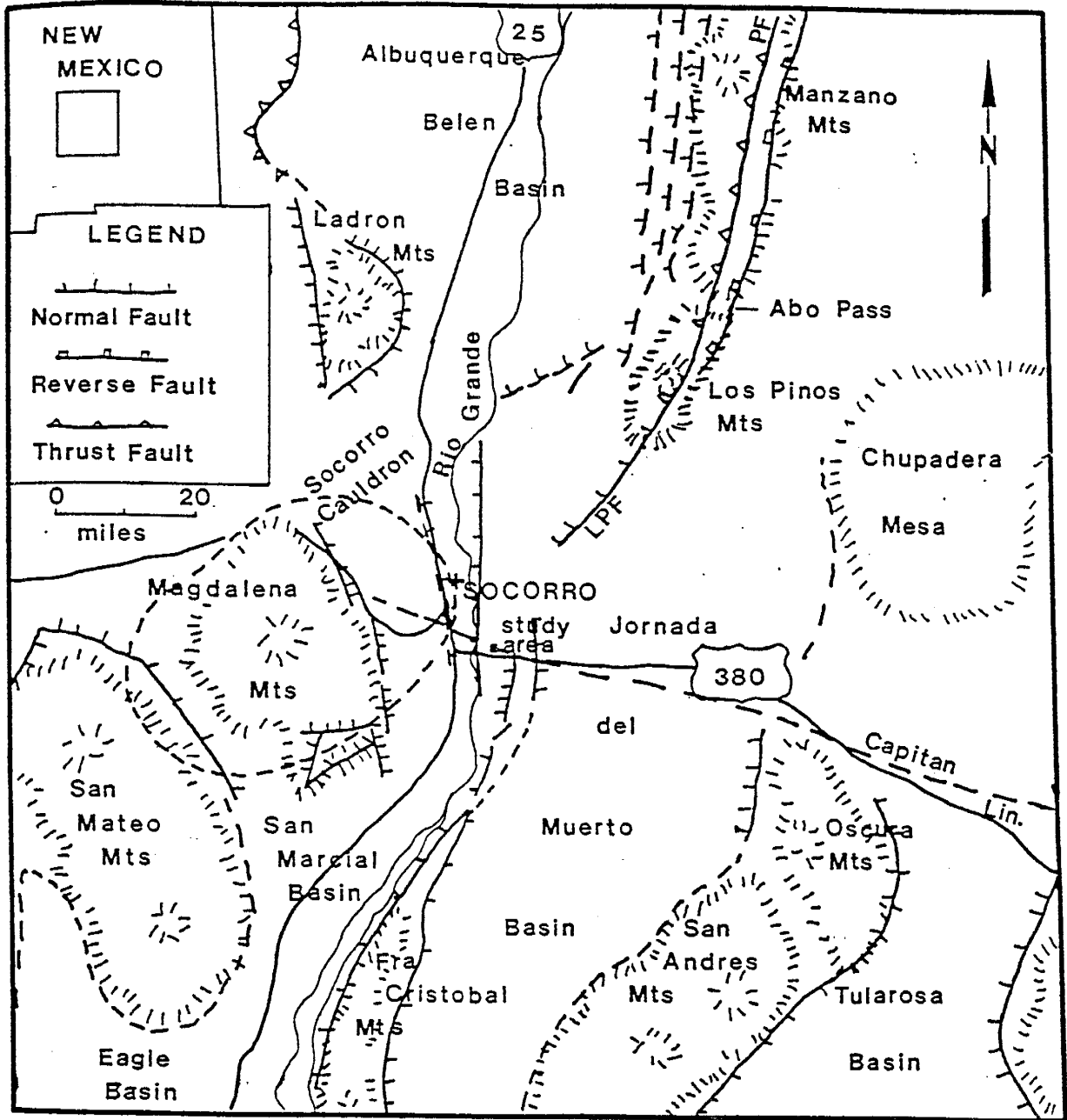


Figure 6. Location of the study area with respect to regional structures. Base map after Christiansen and Kottowski (1972). Structure after deVoogd (1986), Hawley (1978), Yuras (1976), and Chapin (1971).

orientations in his field area. He placed the N-striking faults into two categories based on their relation to the Pliocene to Pleistocene Sierra Ladrones Formation (Bauch, 1982). Category 1 offsets the early Oligocene Spears Formation but not the Sierra Ladrones Formation (Bauch, 1982), whereas category 2 offsets both. Rejas (1965) stated that the N-striking faults were genetically related to the Rio Grande rift. Maulsby (1981) only recognized Rejas's category 2 of the N-striking normal faults in his field area. Bauch (1982) did not mention high-angle faulting in his field area but mapped representatives from all three groups. Fagrelus (1982) was the first to document the northwest-striking, high-angle normal faults.

Low-angle faulting was first proposed by C. T. Smith as early as 1970 (pers. com., 1990) and later confirmed by Maulsby (1981), Bauch (1982), and Fagrelus (1982). These faults usually have dips less than 15° and are most readily recognized in the Permian section. They are most common in the Cañas Gypsum Member of the Yeso Formation and between the Torres and Joyita Members of the Yeso Formation (Cañas tectonically removed). In addition, Fagrelus (1982) found them in the Glorieta and San Andres Formations. Proposed mechanisms for the development of low-angle faults include thrusting, gravity sliding, and reactivation of thrust faults as gravity slides. Recently, for an area around Mesa del Yeso, Linden (1990) supported the gravity slide hypothesis.

In addition to faulting, the region is characterized by several fold styles: (1) tight, overturned folds; (2) broad, open folds; and (3) folds due to drag on fault planes and subsidence of graben blocks. Tight, overturned folding affects Permian and older strata

(Rejas, 1965; Bauch, 1982). Fold axes trend north with vergence towards the east (Bauch, 1982), and northwest with vergence towards the northeast (Rejas, 1965). The tight overturned folds may be related to an uppermost Permian or early Triassic shortening event (C.T. Smith, pers. com., 1990). The broad, open folds primarily affect late Cretaceous strata; however, Bauch (1982) mentioned their existence in the Yeso Formation (Permian), and considered them Laramide in age. Fold axes trend north and gently plunge to the south (Fagrelus, 1982). Group three folds have only been recognized and described by Fagrelus (1982).

It has been suggested by C. T. Smith (pers. com., 1990) that the area has been subjected to a post-uppermost Permian or Early Triassic shortening event. Data presented in this study suggest the possibility of such an event but it cannot be proved conclusively. Mesoscopic folding and related low-angle faulting are confined to upper Pennsylvanian and lower Permian strata, however, the deformation cannot be distinguished from late Cretaceous deformation. In this study, the earliest deformational event has been postulated to be Cretaceous in age.

FOLDS

Folds which occur in the field area are subdivided into two categories based on scale: (1) mesoscopic; and (2) macroscopic. Mesoscopic folds are located in the SW1/4, SW1/4, Sec. 5, T.4 S., R.2 E. and are labelled Fold I in figure 7. Macroscopic folds are located in the eastern and southern parts of the study area and are labelled Fold II, Fold III, Fold IV, and Fold V in figure 7.

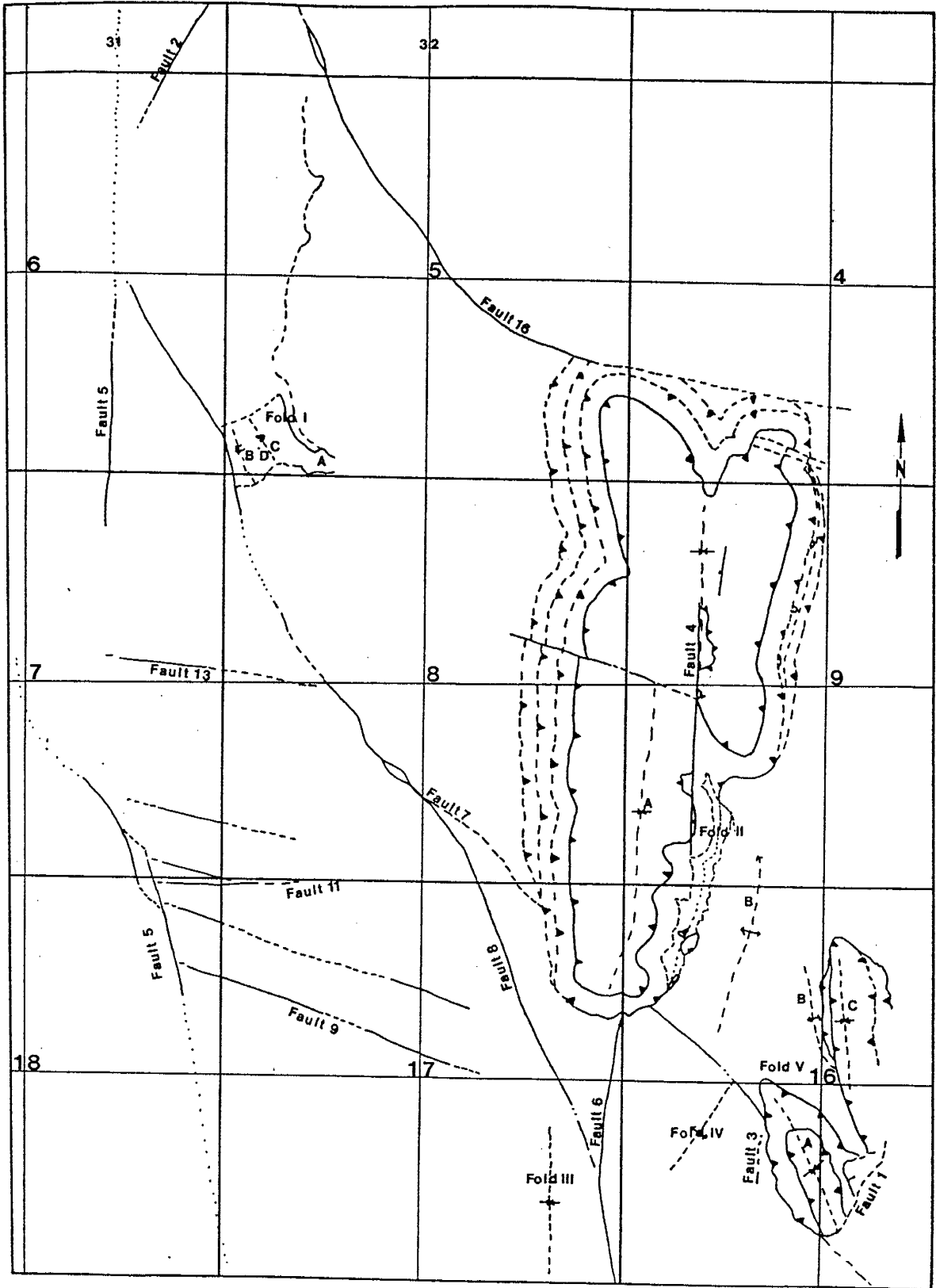


Figure 7. Map of the study area illustrating the locations of structural features.

Mesosopic Folds

The arroyo located in the SW1/4, SW1/4, Sec. 5 provides two good exposures and two excellent exposures of outcrop-scale folds. The two excellent exposures are labelled Fold A and Fold B (Fig. 7). The two good exposures are labelled Fold C and Fold D (Fig. 7) and occur between Folds A and B.

Fold A. Fold A is a gentle, asymmetric fold located at the east end of the arroyo west of Quebradas Road (Fig. 8) and involves strata of upper Meseta Blanca and lower Torres Members of the Yeso Formation. Beds in the northeastern limb strike N25W and dip 52° NE, beds in the southwestern limb strike N22W and dip 13° SW. The fold axis trends approximately N25W. Thickness perpendicular to bedding remains relatively constant throughout the fold. A minor amount of thinning and thickening occurs in the hinge area of the more internal parts of the fold. Beds in the footwall of the low-angle fault strike N26W and dip 14° NE. The fold dies out in both directions parallel to the trace of the axial surface. The folding is not present in the next arroyo to the north or south.

Fold B. Fold B is an open, asymmetric fold (Fig. 9) located approximately 550 m (1800 ft) west of Fold A and involves strata of the Meseta Blanca Member of the Yeso Formation. Beds in the forelimb strike N20W and dip 77° SW, beds in the backlimb strike N20W and dip 11° SW. Ripple marks indicate that beds in the forelimb are overturned. The fold axis trends approximately N20W. Thickness perpendicular to



Figure 8. View to the southeast of Fold A at the base of the duplex in figure 21 (p. 61). V. Herne for scale is approximately 1.5 m tall.



Figure 9. View to the north of asymmetric folding in Meseta Blanca beds. V. Herne for scale is approximately 1.5 m tall.

bedding of some units remains constant. Slickenside striae are parallel to bedding. The fold is not present northwest or southeast of this arroyo.

Fold C. Fold C is an open, symmetric fold (Fig. 10) located 275 m (900 ft) northwest of Fold A and involves strata of the Meseta Blanca Member of the Yeso Formation. Beds in the southwestern limb strike approximately N50W and dip 36° NE, beds in the northeastern limb strike approximately N24W and dip approximately 35° NE. Ripple marks indicate that the backlimb is overturned. Slickenside occurrences are parallel to bedding. This fold dies out 152 m (500 ft) northwest of the arroyo.

Fold D. Fold D is a close, symmetric fold (Fig. 11) located 92 m (300 ft) south of Fold C and involves strata of the Meseta Blanca Member of the Yeso Formation. The fold occurs towards the left of the figure. The axis of this fold is inclined and the fold is overturned toward the northeast.

Drag Folds. Drag folding occurs in the footwall of the thrust faults. These folds are asymmetric and overturned to the northeast. Wavelengths are up to 18 cm. Fold axes trend approximately N30W. The backlimbs have dips of 14° SW and forelimbs have dips of approximately 64° NE. Drag folds developed in incompetent beds form fold trains (Fig. 12a), whereas those developed in competent beds form one cycle (Fig. 12b).

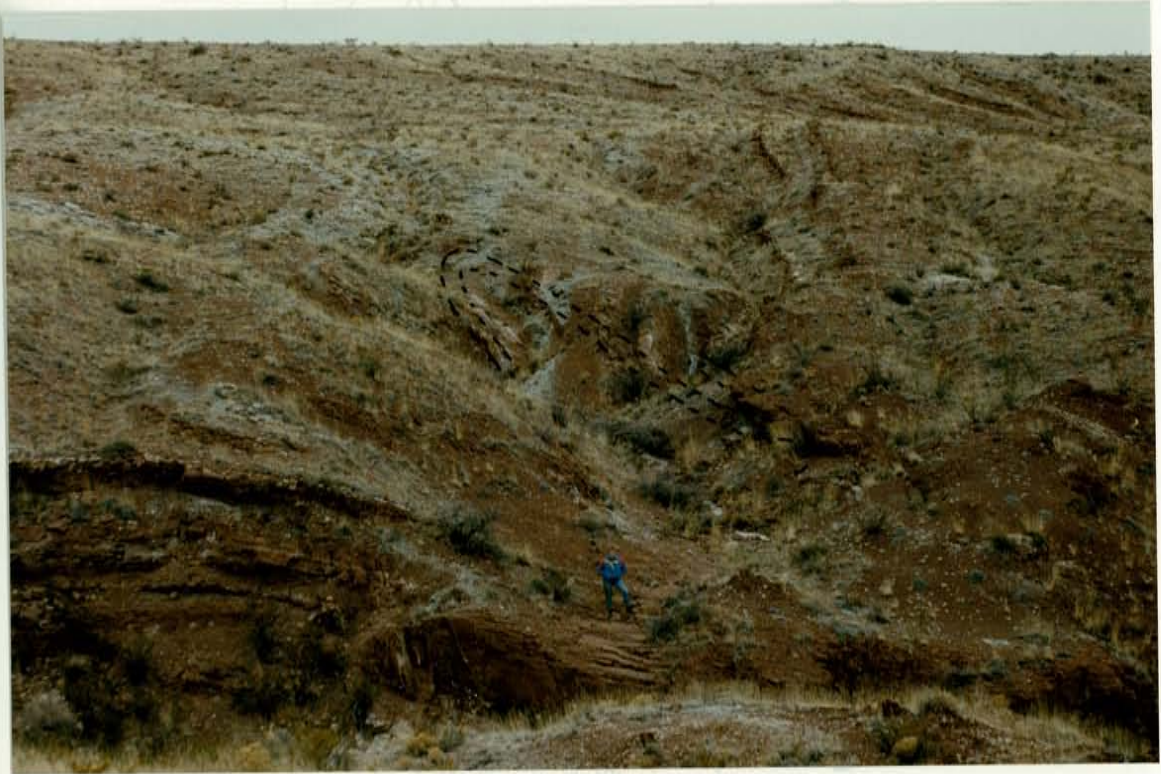


Figure 10. View to the northwest of folds within Meseta Blanca beds overturned to the southwest. V.

Herne for scale is approximately 1.5 m tall. SW1/4, SW1/4, Sec. 5.

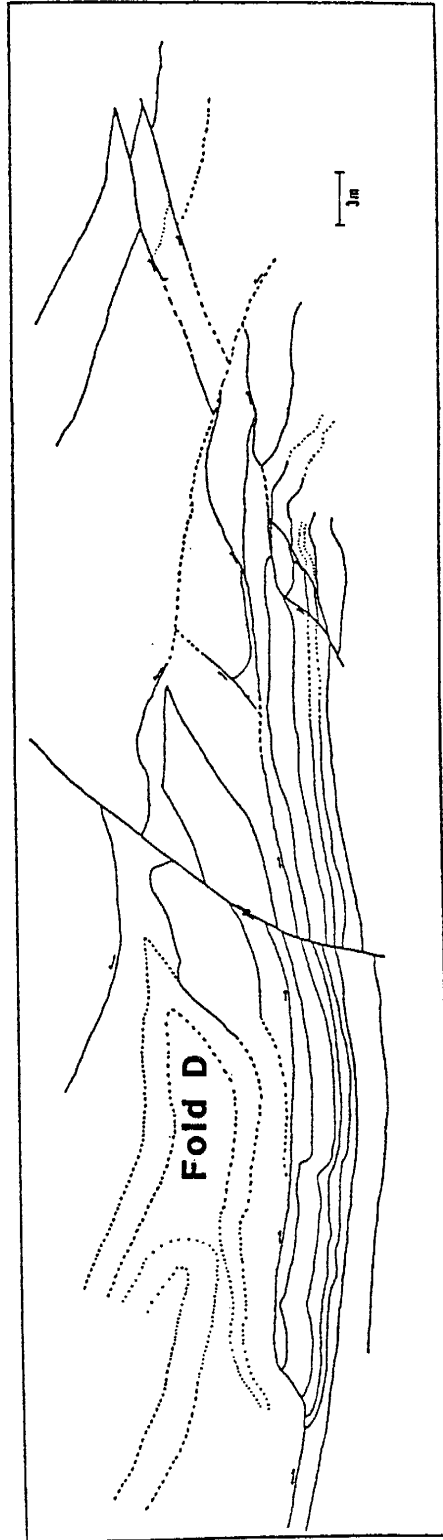


Figure 11. Sketch of composite photograph of imbricate system in the SW1/4, SW1/4, Sec. 5. Also shown is Fold D.



Figure 12a. View to the northwest of fold train in footwall of a thrust; SW1/4, SW1/4, Sec. 5. Folds are developed in incompetent beds of the Torres Member. Pen for scale is 15 cm long.



Figure 12b. View to the northwest of a single drag fold in the footwall of a small ramp; SW1/4, SW1/4, Sec. 5. Fold developed in a competent bed of the Meseta Blanca Member. Pen for scale is 15 cm long.

Macroscopic Folds

The macroscopic folds consist of seven map-scale, gently plunging synclines or anticlines. Fold II consists of a broad syncline exposed in the eastern ridge labelled Fold A and a broad anticline located in the NW1/4, Sec. 16, T.4 S., R.2 E. labelled Fold B. Fold III is an asymmetric syncline (angle) located in the SE1/4 Sec. 17, T.4 S., R.2 E.. Fold IV is an asymmetric anticline (angle) located in the in the NW1/4, SW1/4, Sec. 16, T.4 S., R.2 E.. Fold V is located in the NE1/4, SW1/4, Sec. 16, T.4 S., R.2 E..

Fold II. The gentle, syncline-anticline system associated with Fold II involves Pennsylvanian through upper Triassic strata, but is best seen in the San Andres and Glorieta Formations. The eastern ridge is composed of a large faulted syncline (Fig. 13) and is labelled Fold A. Fold B exposed within the Torres beds on the southeast side of the ridge is an eroded plunging anticline (Fig. 14). These folds were analyzed separately by equal-area projection. Both folds are cylindrical and plunge approximately 2° toward the north. The axis of Fold A trends N02W, the axis of Fold B trends N08E. Fold A is continuous to the north. Fold B is offset by Fault 7 to the south and possibly continues north to Fault 16.

Fold III. Fold III is a gentle, asymmetric syncline located in the SW1/4, Sec. 17. Folding is observed in strata of the Meseta Blanca Member of the Yeso Formation. Strata within the E1/3, SE1/4, Sec. 17 strike toward the northwest and dip steeply to the southwest (average of 43°). Strata within the remainder of the quarter section strike



Figure 13. View to the north of ridge in eastern part of area showing synclinal structure.



Figure 14. View to the northeast of the nose of an anticline plunging to the north; NE1/4, NW1/4, Sec. 16. Fold developed in Torres Member of the Yeso Formation.

northeast and dip gently southeast (average of 15°). Equal-area projection gives a plunge and trend of 6° S06E for the fold axis and indicates that the fold is cylindrical.

Fold IV. Fold IV is a gentle, asymmetric anticline (Fig. 15) located in the SW1/4, Sec. 16 approximately 152 m (500 ft) south of the road and involves strata of the Abo Formation. Beds within the forelimb strike N30E and dip 60° NW, beds in the backlimb strike N30E and dip 14° SE. Equal-area projection indicates that the fold is cylindrical and has a plunge and trend of 0° S45W. The northeastern end of the fold is offset by Fault 7, the fold dies out to the southwest. The fold was traced for 427 m (1400 ft).

Fold V. Fold V contains three gentle, asymmetric to symmetric folds. The folds are located in central Sec. 16 and are labelled A to C (Fig. 7).

Fold A: Fold A is a gentle, asymmetric syncline located in the NE1/4, SW/14, Sec. 16. Beds in the forelimb strike approximately N30W and dip approximately 25° NE, beds in the backlimb strike approximately N30W and dip approximately 15° SW. Equal-area projection indicates that the fold is cylindrical and gives a plunge and trend of 3° S25E. the fold was traced for 671 m (2200 ft).

Fold B: Fold B is a gentle, asymmetric anticline located in the SE1/4, NW1/4, Sec. 16. Beds in the forelimb strike approximately N45W and dip approximately 32° SW, beds in the backlimb strike approximately N-S and dip approximately 18° NE. Stereographic projection indicates that the fold is cylindrical and gives a plunge and trend of 4° S42E. The fold was traced for 457 m (1500 ft). The fold is covered by the ridge in north-



Figure 15. View to the southwest of asymmetric fold in the Abo Formation; NE1/4, SW1/4, Sec. 16. C. Beck for scale is approximately 2 m tall.

central Sec. 16.

Fold C: Fold C is a gentle, symmetric syncline located in the SW1/4, NE1/4, Sec. 16. Beds in the southwestern limb strike approximately N10W and dip approximately 15° NE, beds in the northeastern limb strike approximately N10W and dip approximately 16° SW. Stereographic projection indicates that the fold is cylindrical and gives a plunge and trend of 1° N08W. The fold was traced for 1006 m (3300 ft).

FAULTS

Numerous faults occur within the study area. Poles to all fault surfaces have been plotted and contoured on an equal-area projection (Fig. 16). This projection demonstrates that the faults can be divided into three groups based on azimuth and dip. The most numerous faults are the northwest-striking (9 measurements) and the low-angle faults (16 measurements). The concentration of north- and northeast-striking faults is the smallest (6 measurements).

North- and Northeast-striking Faults

North- and northeast-striking faults consist of north-striking and northeast-striking faults that statistically form one concentration. This is mainly due to the small number of faults, but is also related to a small separation in azimuth. Six faults occur in the study area and are labelled 1 through 6 on plate 1.

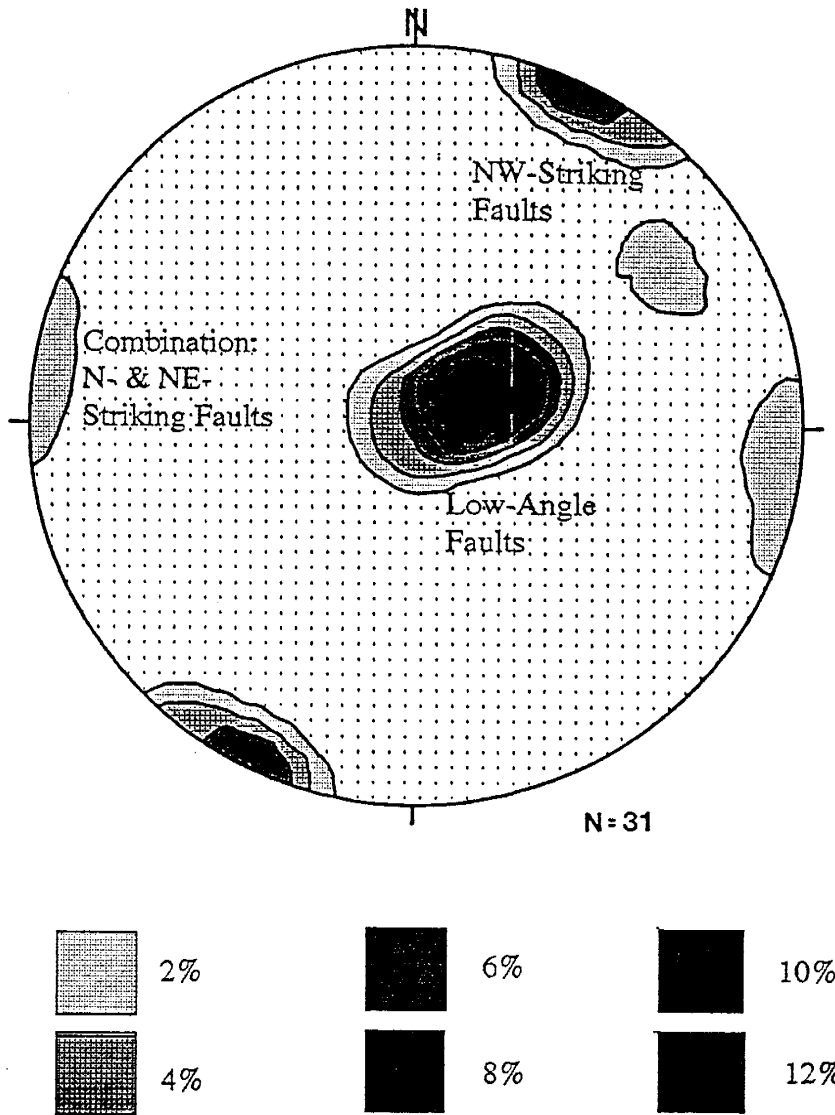


Figure 16. Contoured (1% area) plot (Lambert equal-area net, lower hemisphere projection) of faults within the field area.

Fault 1. Fault 1 is located in the SE1/4, Sec. 16, T.4 S., R.2 E. and separates upthrown Glorieta and San Andres Formations on the northwest from downthrown Santa Rosa Formation on the southeast. The fault can be traced continuously for approximately 457 m (1500 ft), however exposures of the fault surface are rare. At the one locality where the fault surface is exposed it strikes N30°E and dips 30° SE. A component of motion along the fault was normal with a dip separation of approximately 250 m (820 ft).

Fault 2. Fault 2 is located in the southeast part of Sec. 31, T.3 S., R.2 E. and separates upthrown Abo Formation on the southeast from downthrown Meseta Blanca and Torres Members of the Yeso Formation on the northwest. The fault can be traced continuously for approximately 488 m (1600 ft) but exposures of the fault surface are rare. Solution of a three-point problem gives an average strike of N30°E and a dip of 90°. Sense of movement along the fault was down-to-the-northwest with a dip separation of approximately 152 m (500 ft).

Fault 3. Fault 3 is located in the NE1/4, SW1/4, Sec. 16, T.4 S., R.2 E. and offsets the Abo Formation. The fault can be traced continuously for 122 m (400 ft). The fault surface is not exposed. Solution of a three-point problem gives an average strike of N05E and dip of 90°. Sense of movement along the fault was down-to-the-southwest with a dip separation of approximately 12 m (40 ft).

Fault 4. Fault 4 is located in the E1/2, Sec. 8, T.4 S., R.2 E. and separates upthrown San Andres, Glorieta, and Yeso Formations on the east from downthrown San Andres, Glorieta, and Yeso Formations on the west. The fault can be traced continuously for approximately 1037 m (3400 ft) with good exposures of the fault zone along the trace. The fault zone varies in width from .9 m (3 ft) to less than .3 m (1 ft) and consists intermittently of either a gouge zone (Fig. 17) or a breccia that is sometimes associated with travertine veins (Fig. 18). The gouge is a fine white powder. The breccia is 22 cm thick and composed of matrix supported grains of San Andres and Glorieta Formation. Grain size varies from 2.7 cm to .1 cm with an average size of .74 cm. The grains are subangular to subrounded; some of the smaller grains are well-rounded and do not exhibit a preferred orientation. The matrix consists of a zone of botryoidal calcite and a zone of detrital type. All of the grains are rimmed by dark, reddish-brown to light brown iron oxide. The travertine veins are less than 6 cm in thickness. In areas where the fault surface is exposed the strike ranges from N05W to N10W and dips approximately 78° west. Sense of movement along the fault was down-to-the-west with a dip separation of approximately 152 m (500 ft).

Fault 5. Fault 5 is located along the western margin of the field area and separates upthrown Madera and Bursum Formations on the east from downthrown Santa Fe Group on the west. The fault can be traced intermittently for approximately 4.8 km (3 mi) from the SE1/4, Sec 18, T.4 S., R.2 E. to the southeast part of Sec. 31, T.3 S., R.2 E.. Fault surfaces are rarely exposed, but for those exposed the strike varies from N35W to N03E



Figure 17. View to the north of gouge zone of Fault 4 cutting low-angle fault between San Andres and Glorieta Formations. S = San Andres Formation; B = Breccia; and G = Gouge. Hammer for scale is 34 cm long.



Figure 18. Photograph of fault zone (Fault 4) SE1/4, NW1/4, SW1/4, Sec. 9 showing breccia (B) and travertine (T). Pen for scale is 15 cm long and oriented 355°.

and dips 80 to 90° west. Solution of a three-point problem gives an average strike of N07E and a dip of 88° west. A component of motion along the fault was normal.

Fault 6. Fault 6 is located in the E1/8, Sec. 17, T.4 S., R.2 E. and separates upthrown Abo Formation on the east from downthrown Meseta Blanca Member of the Yeso Formation on the west. The fault can be traced continuously for approximately 1098 m (3600 ft) with rare exposures of the fault zone. Solution of a three-point problem gives an average strike of N05E and a dip of 68° west. Sense of movement along the fault was down-to-the-west with a dip separation of approximately 244 m (800 ft). The fault terminates against the Glorieta Formation to the north.

Northwest-striking Faults

Northwest-striking faults are the most common orientation of high-angle faults in the study area. They have been labelled 7 through 16 on plate 1. The isolated 2% concentration of faults in figure 16 is not a minor group, it consists of poles to faults 7, 8, and 16.

Fault 7. Fault 7, located in the northwestern, south-central, and southeastern portions of the map area, separates upthrown Bursum, Abo, and Yeso Formations on the southwest from downthrown Bursum through San Andres Formations, Santa Rosa and San Pedro Arroyo Formations on the northeast. The fault can be traced continuously for approximately 5.1 km (3.1 mi) from SW1/4, NE1/4, NE1/4, Sec. 21, T.4 S., R.3 E.

(south of the map area) to the SW1/4, Sec. 5, T.4 S., R.2 E.. The fault zone is intermittently exposed and varies in width from 1.5 m (5 ft) to 6.1 m (20 ft). In the field the fault zone is predominantly recognized by a juxtaposition of stratigraphic units rather than a breccia zone. Slickenside striae can be found on exposures of Abo Formation in two locations: (1) SW1/4, SW1/4, Sec. 5, T.4 S., R.2 E., and (2) SE1/4, NW1/4, Sec. 16, T.4 S., R.2 E.. The trend of the striae range between N15W, at location 1, and N62W, at location 2. Plunge of the striae range from 0° to 30°. Fault planes strike between N62W and N15W and dips 58° to 90° northeast. Solution of a three-point problem gives an average strike of N25W and a dip of 70° northeast. Motion along the fault was oblique with a dip separation of approximately 455 m (1460 ft) and a strike separation of approximately 732 m (2400 ft).

Striae observed where the fault truncates the steep forelimb of Fold IV is a relatively small area (137 m (450 ft) by 31 m (100 ft); labelled **A1** on the map) characterized by siltstones of the Abo Formation deformed by both Fault 7 and folding. This deformation has led to the formation of three principal sets of slickenside surfaces. Trend and plunge measurements of striae are shown in figure 19a. Because striae associated with Fault 7 are small in number and obscured by other surfaces, a scatter diagram (Fig. 19a) and a contoured plot (Fig. 19b) have been prepared to separate the lineations.

Fault 8. Fault 8 is located in the NE1/4, Sec. 17, T.4 S., R.2 E. and offsets the Meseta Blanca Member of the Yeso Formation; east side is down. The fault can be

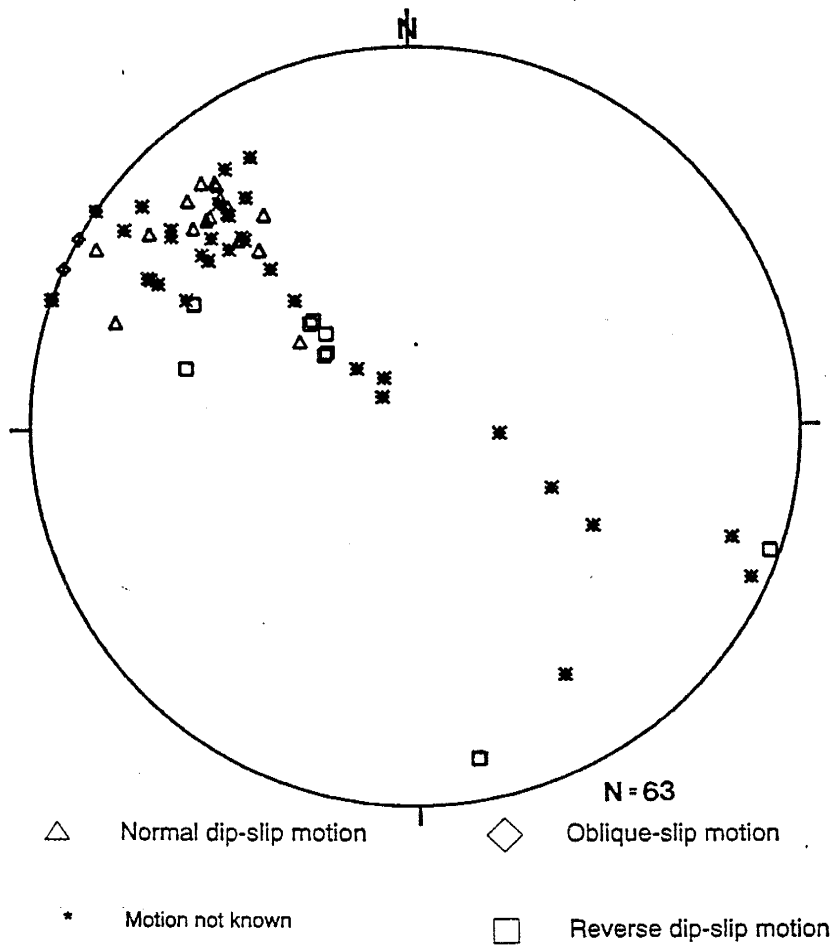


Figure 19a. Scatter diagram (Lambert equal-area net, lower hemisphere projection) of slickenside striae orientations in Area 1 showing type of motion. Great circle represents orientation of Fault 7.

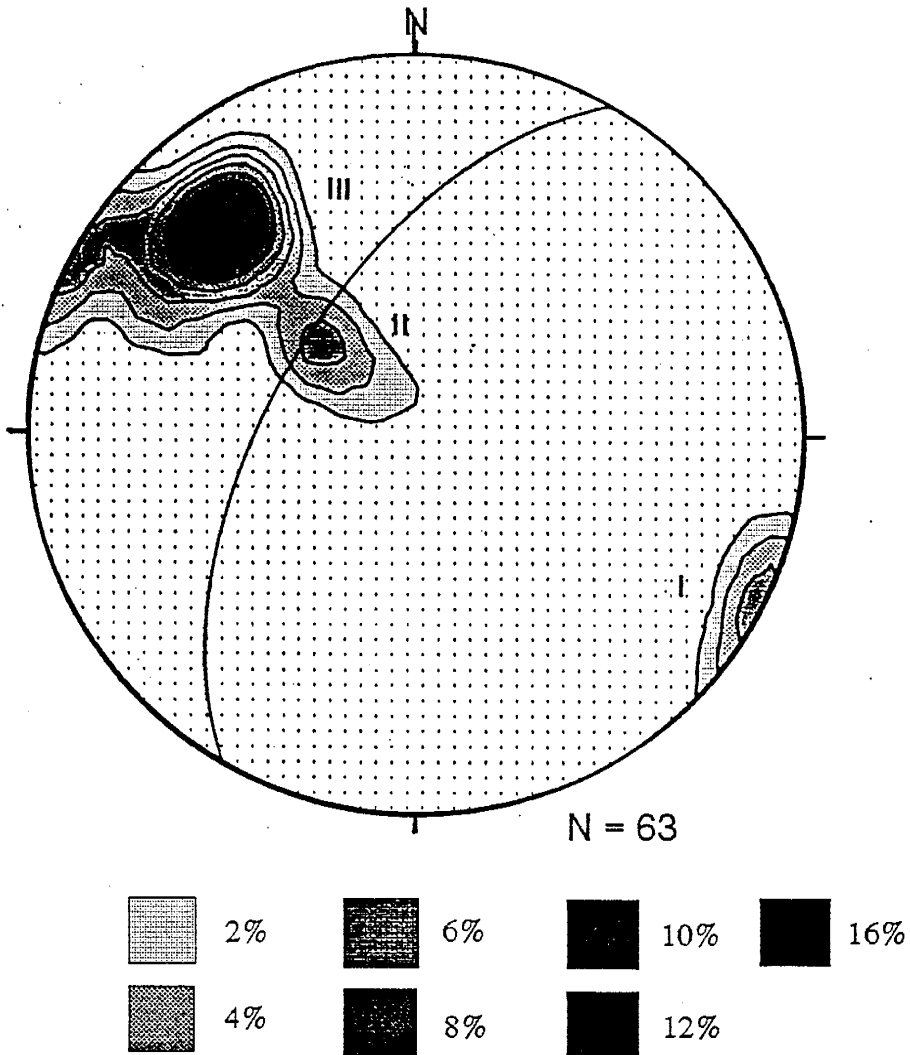


Figure 19b. Contoured (1% area) plot (Lambert equal-area net, lower hemisphere projection) of data in figure 19a showing three areas of concentration (labelled I through III). Great circle represents orientation of bedding in Area 1.

traced continuously for approximately 1494 m (4900 ft) with no exposure of a fault surface. The fault trace is identified by the absence of part of the Meseta Blanca section. Solution of a three-point problem gives an average strike of N20W and a dip of 63° northeast. Sense of motion along the fault was down-to-the-northeast with a dip separation of approximately 62 m (200 ft).

Faults 9 - 13. Faults 9 - 13 are located in the southwest corner of the study area and separate upthrown Madera, Bursum, and Abo Formations on the southwest from downthrown Madera, Bursum, and Abo Formations on the northeast. The faults can be traced intermittently from 701 m (2300 ft) to 1280 m (4200 ft) with minimal exposures of fault surfaces. The fault zones are characterized by the juxtaposition of different parts of the stratigraphic section. In the few areas where fault surfaces are exposed, slickenside striae are present. The fault striae trend between north-south and N40W and plunge 90°. From solution of three-point problems, the strikes range from N60W to N70W and dip 90°. A component of motion was normal with stratigraphic throw varying between approximately 9 m (30 ft) (Fault 9; Plate 1) to approximately 61 m (200 ft) (Fault 10; Plate 1).

Fault 14. Fault 14 is located in the NE1/4, Sec. 8, and the SW1/4, NW1/4, Sec. 9, T.4 S., R.2 E. and separates upthrown upper Yeso, Glorieta, and San Andres Formations on the northeast from downthrown upper Yeso, Glorieta, and San Andres Formations on the southwest. The fault can be traced continuously for 793 m (2600 ft). The fault

appears to die out towards the east side of the ridge. The fault zone is approximately 1.5 m (5 ft) to 3 m (10 ft) wide and is characterized by the juxtaposition of units in the upper Yeso and Glorieta Formations and by calcite filled veins within the San Andres Formation. Solution of a three-point problem gives an average strike of N72W and dip of 90°. Sense of movement along the fault was down-to-the-northeast with a maximum stratigraphic throw of approximately 30 m (100 ft).

Fault 15. Fault 15 includes two small faults located in the SE1/4, SW1/4, Sec. 4, T.4 S., R.2 E. and offsets the San Andres and Glorieta Formations and the Torres Member of the Yeso Formation. The faults can be traced continuously for approximately 213 m (700 ft) with poor exposure of fault surfaces. Solution of a three-point problem gives an average strike of N70W and a dip of 90°. Motion along the faults had a normal component with a stratigraphic throw of approximately 9 m (30 ft). The northern fault is down-to-the-northeast and the southern fault is down-to-the-southwest, resulting in a horst structure.

Fault 16. Fault 16 is located in the northeastern portion of the study area and separates upthrown Bursum, Abo, and Yeso Formations on the northeast from downthrown Bursum, Abo, and Yeso Formations on the southwest. The fault can be traced continuously for approximately 2.8 km (1.7 mi) from the SW1/4, Sec. 4, T.4 S., R.2 E. to the southwestern portion of Sec. 32, T.3 S., R.2 E.. Good exposures of the fault zone occur along the length of the trace. The width of the zone varies from 3 m (10 ft)

to 6 m (20 ft) and is characterized by a breccia zone (Fig. 20). The breccia consists of matrix supported fragments of Torres limestone. Fragments are angular to subrounded and show no preferred orientation. Grain size varies from 7.6 cm to .2 cm. In many places the breccia can be found in contact with siltstones of the Meseta Blanca Member of the Yeso Formation and Abo Formation but these units were not involved in the brecciation. At the one locality where the fault surface is exposed it strikes N30W and dips 67° northeast. Solution of a three-point problem gives an average strike of N43W and a dip of 72° northeast. Motion along the fault was oblique with a dip separation of approximately 366 m (1200 ft) and a strike separation of approximately 1.4 km (4600 ft).

Low-Angle Faults

The low-angle faults can be divided into two groups based on the type of age relationship they display: (1) older beds over younger; (2) younger beds over older.

Faulting which places older rocks over younger was found only in the SW1/4, SW1/4 Sec. 5 T.4 S., R.2 E. At the scale these structures are observed, they can be called thrust faults. Faulting which brings younger rocks over older occurs in the eastern ridge, and smaller ridges in the SW1/4 of Sec. 16.

Terminology used within this section is from Boyer and Elliott (1982), Butler (1982), Morley (1986), Washington (1987), and Dunne and Ferrill (1988). A **thrust sheet** is a volume of rock bounded below by a thrust fault. A useful convention is to name the thrust sheet after this underlying or leading thrust fault. An **imbricate system** (or Schuppen structure) occurs when each thrust in a system repeats the size and shape



Figure 20. View to the northwest of breccia zone (left half) related to movement along Fault 16.

Right half of the photo is Meseta Blanca Member of the Yeso Formation. Dog for scale is .6 m tall.

of the neighboring thrust so that the thrust sheets overlap like roof tiles, all dipping in the same direction. **Duplexes** are anastomosing systems of thrusts in which the various imbricate faults branch off a common basal (floor) fault surface and join a common overlying (roof) thrust surface. The fault-bounded blocks within the duplex are termed **horses**.

Older beds over younger

Thrust faults located in the SW1/4, SW1/4, Sec. 5, T.4 S., R.2 E. were observed at Stop 5 of the "First Day Road Log" in the NMGS Guidebook 34 (Smith et. al., 1983; page 19). Faults strike, on average (see Table 1), N26W and dip to the southwest. Ramps have dips of about 18° - 37° and flats range from 2° - 4° to the southwest. Rare fault striae (imbricate system, Fig. 11, p. 38) have a plunge and trend of 16° S47W. Steps on the striae as well as stratigraphic offset indicate reverse motion.

The structure exposed at the eastern end of the arroyo is a small duplex with thrust related folding (Fig. 21). The roof thrust of this duplex ramps down into the arroyo just to the right of the figure where it joins the floor thrust. About 152 m (500 ft) west of the duplex is a flat-ramp geometry in the south wall (Fig. 22). Where the arroyo bends south is the start of an imbricate system . This system is best exposed in the west wall (Fig. 11). The floor thrust of this system is located approximately 2 ft from the arroyo bottom. At the south end of the system, where the arroyo starts bending to the west, is a ramp coming out of the arroyo from which the floor thrust of the system branches separating the folding which is encountered around the bend (Fig. 9, p. 35)



Figure 21. View to the southeast of duplex at the east end of the arroyo, west of Quebradas Road;
SW1/4 SW1/4 Sec. 5. V. Herne for scale is approximately 1.5 m tall.



Figure 22. View to the south of small ramp-flat geometry in the Meseta Blanca Member of the Yeso Formation; SW1/4, SW1/4, Sec. 5. Isaac for scale is approximately 1.7 m tall.

from the rest of the system.

Table 1. Strike and dip of thrust faults measured from east to west in arroyo in SW1/4,SW1/4, Sec. 5.

LOCATION	STRIKE	DIP
Duplex (Fig. 21)		
	N28W	32 SW
	N25W	16 SW
	N22W	04 SW
	N22W	19 SW
	N15W	28 SW
	N15W	22 SW
	N15W	02 SW
	N23W	03 SW
Small flat-ramp system (Fig. 22)		
	N30W	18 SW
	N30W	02 SW
Imbricate system (Fig. 11, p. 38)		
	N40W	18 SW
	N40W	18 SW
	N32W	27 SW
	N30W	24 SW

This arroyo appears to cut a small thrust sheet (see mesoscopic fold analysis) which has been offset by Fault 7 on the west and it is not known how far to the east it extends.

Younger beds over older

In the study area, faulting which places younger beds over older beds occurs in two areas: 1) the eastern ridge; and 2) northwest-trending ridges in central Sec. 16, T.4 S., R.2 E. (hereafter referred to as the 'southeastern ridges'). The fault surfaces are

coincident with bedding planes with dips ranging from 8° to 19°. They occur at several stratigraphic levels: 1) between the Torres and Cañas Members of the Yeso Formation; 2) between the Cañas and Joyita Members of the Yeso Formation; 3) between the Joyita Member of the Yeso Formation and the Glorieta Formation; 4) between the Torres member of the Yeso Formation and the Glorieta Formation (Cañas and Joyita tectonically removed), 5) between the Glorieta and San Andres Formations; and 6) between the Torres Member of the Yeso Formation and the San Andres Formation (Cañas and Joyita and the Glorieta Formations tectonically removed).

Eastern Ridge. Within the first area there are four structural levels of low-angle faults: one between the Torres Member and the Cañas Member of the Yeso Formation; one between the Cañas Member and the Joyita Member of the Yeso Formation; one between the Joyita Member of the Yeso Formation and the Glorieta Formation; and one between the Glorieta and San Andres Formations. The fault surface between the Glorieta and San Andres Formations can be observed in many locations. Recognition of fault surfaces between the Joyita Member of the Yeso Formation and the Glorieta Formation, and between the Cañas and Joyita Members of the Yeso Formation are based on anomalously thin exposures of these units at different locations. Both units thin, structurally, towards the southeast from approximately 31 m to 0 m (100 to 0 ft). The fault between the Torres and Cañas Members of the Yeso Formation is deduced from the outcrop pattern.

On the west side of the ridge, low-angle faults can be traced from the north, where they appear to cover Fault 16, towards the south; one minor northwest-striking

fault (Fault 14) offsets the low-angle faults along this trace. In the NW1/4, NE1/4, NE1/4 Sec. 17, T.4 S., R.2 E. the lower fault 'ramps' upsection cutting out the Cañas and Joyita Members of the Yeso Formation and bringing the Glorieta Formation into fault contact with the Torres Member of the Yeso Formation. On the southeast side of the ridge the Glorieta Formation remains in fault contact with Torres limestones. On the east side of the ridge it appears that the Glorieta Formation is still in fault contact with Torres limestones. However, to the north, small pods of gypsum are present (Fig. 23). These gypsum pods are interpreted to be Cañas, because of outcrops of Joyita Sandstone above some of the pods (e.g. NE1/4, SW1/4, NE1/4, Sec. 16, T.4 S., R.2 E.). In the NE1/4, SW1/4, Sec. 9, T.4 S., R.2 E. the Glorieta Formation is in fault contact with limestones of the Torres member for a distance of 244 m (800 ft). To the north, pods of Cañas gypsum and Joyita sandstone crop out (both of these units are thinned on the east side of the ridge compared to the west side). In the SE1/4, SW1/4, Sec. 4, T.4 S., R.2 E., the Torres limestones are again in fault contact with the Glorieta Formation. The single fault continues north to the NE1/4, SW1/4, Sec. 4, T.4 S., R.2 E., where it ramps down exposing the Cañas and Joyita Members of the Yeso Formation.

A low-angle fault between the Glorieta and San Andres Formations is well exposed along the length of the trace. This fault strikes on average N28E with an average dip of 19° NW. The contact can be observed in many locations and consists of two types of breccia zones. **Type I** contains fragments of the Glorieta and San Andres Formations (Fig. 24). **Type II** occurs within the San Andres Formation and only contains fragments of the San Andres Formation (Fig. 25). Individual fragments are



Figure 23. View to the northwest of low-angle fault surfaces of the east side of the ridge. **S** = San Andres Formation; **G** = Glorieta Formation; **J** = Joyita Member, Yeso Formation; **C** = Cañas Member, Yeso Formation; and **T** = Torres Member, Yeso Formation.



Figure 24. View to the southwest of a Type I breccia showing clasts of the Glorieta (G) and San Andres (S) Formations. Hammer for scale is 34 cm long.



Figure 25. View to the northwest of a **Type II** breccia NW1/4, NE1/4, Sec. 16. Knife for scale is 28 cm long.

angular to subrounded and show no preferred orientation. Both types of breccia zones range in thickness from approximately 6 m (20 ft) to less than .03 m (1 in.) and are matrix supported. The matrix of a **Type I** breccia is detrital, whereas the matrix of a **Type II** breccia is calcareous. Both types of breccias are poorly to very poorly sorted, but the size of the fragments depends on the thickness of the zone.

Type I. Grain size within a 1.8 m (6 ft) thick zone exposed in the NW1/4, NW1/4, SW1/4, NW1/4, Sec. 16, T.4 S., R.2 E. varies from approximately 61 cm to 2.54 cm. The average grain size is 26 cm and the phi standard deviation (Folk, 1974) is greater than 2.0 (very poorly sorted). Grain size within a .6 m (2 ft) thick zone exposed in the SE1/4, NW1/4, SW1/4, Sec. 9, T.4 S., R.2 E. varies from approximately 26 cm to 1.3 cm. The average grain size is 14 cm and the phi standard deviation is greater than 2.0.

Type II. Grain size within a 3.7 m (12 ft) thick zone exposed in the NW1/4, SW1/4, NW1/4, NE1/4, Sec. 16, T.4 S., R.2 E. varies from approximately 90 cm to 15.25 cm. The average grain size is 53 cm and the phi standard deviation is between 1.0 and 1.5 (poorly sorted). Grain size within a 4 cm thick zone exposed locally at the top of the previous zone varies from approximately .4 cm to .06 cm. The average grain size is .23 cm and the phi standard deviation is between 1.0 and 1.5.

Although it is difficult to determine where in the section the fault occurs, the fact that it exists at different stratigraphic levels in different locations can be established by tracing a distinctive sandstone horizon within the San Andres Formation. This sandstone is approximately 1.5 m (5 ft) thick and is probably a tongue of the Glorieta Formation.

In the SW1/4, SE1/4, NW1/4, SW1/4, Sec. 9, T.4 S., R.2 E. it crops out 6 m (20 ft) above the contact; in the NE1/4, NE1/4, NW1/4, SW1/4, Sec. 9, T.4 S., R.2 E., it crops out on the contact.

Southeastern Ridges. There are two structural levels of low-angle faults within this area. The ridge in south-central Sec. 16 exposes faulting between the Torres Member of the Yeso Formation and the Glorieta Formation and between the Glorieta Formation and the San Andres Formation. The ridge in north-central Sec. 16 has outcrops of low-angle faulting between the Glorieta Formation and the San Andres Formation, and between the Glorieta Formation and the Torres Member of the Yeso Formation. Fault-bounded pods of the Glorieta Formation crop out on the west side of the ridge. The two pods observed are less than 31 m (100 ft) in the longest dimension, and are therefore not shown on the map.

Delineation of low-angle faulting between the Glorieta Formation and the San Andres Formation is based on stratigraphy rather than structure. At the base of the San Andres Formation on the south-central ridge is a limestone unit approximately 2 m (6 ft) thick. The base of this unit consists of a .3 m (1 ft) thick micrite overlain by a .6 m (2 ft) thick sequence of thinly bedded fractured micrite. A fossiliferous zone about 18 cm thick overlies the thin-bedded micrites. Fossils are predominantly brachiopods and some minor mollusc fragments. In many places the lower .9 m has been tectonically removed, and in some places the fossiliferous horizon is on the Glorieta Formation. The contact on the eastern side of the ridge in north-central Sec. 16 is not well exposed. Where it

is exposed the same relationship exists, however, the units involved are not equivalent. In one place a 15 cm thick micrite layer is truncated by a small warp on top of the Glorieta Formation. Approximately 24 m (80 ft) above the contact on the northeastern side of the ridge is a low-angle fault within the San Andres Formation (Fig. 26). The fault strikes N80E and dips 19° SE (ramp; flat is covered). The fault surface is about 5 cm thick and is calcite filled. In some places directly beneath the fault a **Type II** microbreccia (4 cm thick) can be found. Underneath this microbreccia is a **Type II** megabreccia approximately 6 m (20 ft) thick. Mineralized surfaces in the fault plane show slickenfibers which have a plunge and trend of 20° S75E. Slickenfiber surfaces step down towards the northwest.

Low-angle fault between the Torres Member of the Yeso Formation and the San Andres Formation and the Torres Member and the Glorieta Formation is inferred from the absence of units. The contact between the Glorieta Formation and the Torres Member is rarely exposed. Where it can be observed, no breccia occurs.

Silica Crystallite Geothermometry

Silica crystallite geothermometry was not a major emphasis of the present study. Most of the research was done as part of a class directed by Dr. Jacques Renault of the New Mexico Bureau of Mines and Mineral Resources. Any person wishing to obtain details of the method can contact either Jacques Renault or myself.

Chert collected from the study area was analyzed using silica crystallite geothermometry to determine the effects of tectonism on the thermal regime experienced



Figure 26. View to the northwest of low-angle fault in the San Andres Formation, NW1/4, NE1/4, Sec. 16. Dead tree, bottom right, is approximately 1.5 m tall.

by the rocks. The method (Renault, 1980) is based on the fact that most naturally occurring crystals are imperfect and consist of what have been called a mosaic (Cullity, 1978; Renault, 1980) or crystallite (Klug and Alexander, 1974; Renault, 1980) structure. The size of the crystallites can be determined by x-ray diffraction peak broadening. From the size, the maximum temperature the sample has experienced can be calculated using a calibration equation. The assumptions for the method are: 1) the growth of the chert began as opaline silica in the form of a gel; 2) the chemical composition is uniform; and 3) heating times were sufficiently long to obtain thermal equilibrium.

The atoms in a crystal consisting of a mosaic structure are not arranged in a perfectly regular lattice extending from one side of the crystal to the other. Instead, the lattice is broken up into a number of domains (mosaic blocks), each slightly misoriented with respect to the others (Fig. 27). Individual domains have dimensions that range in size up to several thousand angstroms, while the maximum angle of disorientation (Cullity, 1978) between them may vary from a very small value to as much as one degree, depending on the crystal. The effect of the mosaic structure is to broaden the diffraction profile. This broadening component (pure diffraction broadening) is separated from components resulting from mechanical aspects of the diffractometer (Klug and Alexander, 1974) by x-ray line deconvolution methods. Pure diffraction broadening increases both with decreasing crystallite size and increasing internal strain (Renault, 1980). Because most micro-crystalline quartz samples have little or no natural or artificially induced internal strain (Klug and Alexander, 1974; J. Renault, pers. com., 1991) this observed pure diffraction broadening is attributable almost wholly to the size

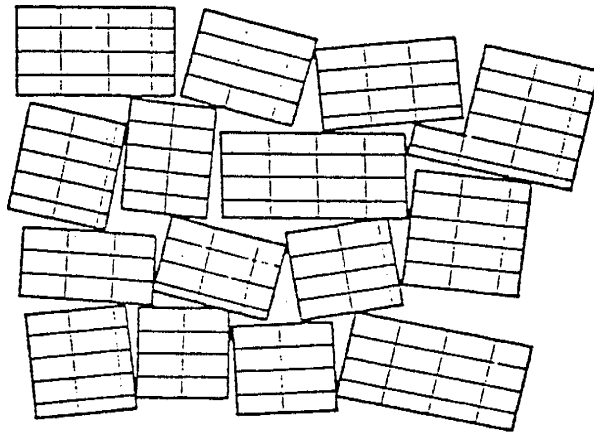


Figure 27. The mosaic structure of a real crystal (after Cullity, 1978).

of the individual domains.

A sample from the San Andres Formation north of Quebradas Road was collected from a bedded chert approximately 1.6 m (5 ft) above the San Andres, Glorieta contact. The sample was unusual in that the limestone immediately underlying the bedded chert had been silicified. The temperature measured from the chert was 230 °C and from the silicified limestone was 260 °C. Temperature measurements on Pennsylvanian nodular chert averaged 200 °C. Temperature measurements on nodular chert within the San Andres Formation south of Quebradas Road and from the Torres Member of the Yeso Formation have a range from 322 °C to 433 °C (F.M. Craig, unpub. data).

Other Structures

Other structures observed but not examined in detail are folding (Fig. 28) and low-angle faulting (Fig. 29) within the Madera Formation in Sec. 17. Both of the structures trend southeast-northwest and probably are related to structures observed in the arroyo in the SW1/4, SW1/4, Sec. 5.

STRUCTURAL ANALYSIS

Mesosopic Fold Analysis

Fold A. Orthogonal thickness of the fold remains relatively constant suggesting it is a parallel fold (Ramsay, 1967). Because no evidence of bedding parallel shear was observed, the fold could have formed by an orthogonal flexure mechanism (Twiss and Moores, 1992). Folding is confined to upper Meseta Blanca and lower Torres Members



Figure 28. View to the southwest of mesoscopic folds in the Madera Formation, Sec. 17.



Figure 29. View to the northwest of low-angle faulting in the Madera Formation, Sec. 17. C. Smith for scale is approximately 1.7 m tall.

of the Yeso Formation suggesting a middle Permian deformation event. However, upper Permian strata may not have been affected due to the size of the fold. The fold dies out toward the north and south.

Fold B. Orthogonal thickness of the fold remains relatively constant in the competent layers of the fold, but the incompetent layers show significant variation. Constant orthogonal thickness in the competent units suggest that the fold is parallel (Ramsay, 1967). Slickenside striae parallel to bedding suggests a bedding-parallel shear. The fold could have formed by a flexural shear mechanism (Twiss and Moores, 1992). Folding is confined to the Meseta Blanca Member of the Yeso Formation perhaps suggesting a middle Permian deformational event.

Fold C. The entire fold is not exposed so thickness relationships cannot be determined. Slickenside striae parallel to bedding suggest a bedding parallel shear, the fold could have formed by a flexural shear mechanism (Twiss and Moores, 1992). Folds formed by flexural fold mechanisms are usually parallel (Twiss and Moores, 1992). Folding is confined to the upper Meseta Blanca Member of the Yeso Formation.

Macroscopic Fold Analysis

The similar orientations and styles of Fold II, Fold III, and Fold V suggest a genetic relationship. Projection of outcrop data into subsurface suggests that orthogonal thickness remains constant, except for units bounded by low-angle faults, suggesting they

are parallel folds (Ramsay, 1967). No evidence of bedding parallel shear was observed suggesting the folds could have formed by an orthogonal flexure mechanism (Twiss and Moores, 1992). The folds affect Madera Formation through San Pedro Arroyo Formation suggesting a post-upper Triassic deformational event. The east limb of Fold III was probably steepened as a result of movement on Fault 6. Smaller folds observed in the Torres member of the Yeso Formation are probably parasitic to the larger fold.

Fold IV does not fit into the typical north-south trend of the area. Orthogonal thickness of the fold remains relatively constant, except in the hinge area which has been thickened by thrusting, suggesting the fold is parallel (Ramsay, 1967). Slickenside striae parallel to bedding (see Fig. 19b; p. 55) suggests a bedding parallel shear; the fold could have formed by a flexural shear mechanism (Twiss and Moores, 1992). Folding is confined to the middle Abo Formation.

Origin of Folds

All of the folds discussed can be attributed to a flexural folding mechanism. Flexural folding of strata can result from bending and/or buckling forces (Twiss and Moores, 1992).

The folds belonging to Fold I occur in close proximity to the small thrust sheet in the SW1/4, SW1/4, Sec. 5. Because of this close association, the formation of these folds may be related to the thrust sheet. Folds that show relatively constant orthogonal thickness are common in foreland fold-and-thrust belts (Twiss and Moores, 1992).

Three types of folds are commonly found in fold-and-thrust belts (Suppe, 1983;

Jamison, 1987; Suppe and Medwedeff, 1990). These are : (1) fault-bend folding (Fig. 30a); (2) fault-propagation folding (Fig. 30b); and (3) detachment folding (Fig. 30c). In many cases, fault-bend folds can be distinguished from fault-propagation folds based on geometry. Fault-bend folds commonly have interlimb angles greater than 100° (Suppe, 1983; Jamison, 1987), whereas fault-propagation folds commonly have interlimb angles less than 100° (Suppe and Medwedeff, 1990). Without knowledge of the thrust geometry it is impossible to distinguish, with certainty, between fault-propagation and detachment folds (Jamison, 1987).

Two of the folds located in this area, Folds A and B, can be described using the theory of fault-propagation folding. The theory is applied in order to determine if the folds are related to the thrust faulting. In addition, because the theory describing fault-propagation folding (Suppe and Medwedeff, 1990) is derived from balanced models, a fold-thrust system displaying the same or similar geometric relationships will be balanced (Jamison, 1987). Because some readers may not be familiar with this type of folding the characteristics are presented prior to a discussion.

A fault-propagation fold is defined as a fold "that forms and grows at the tips of thrust faults. As a fault continues to propagate, the fold continues to grow at the fault tip" (Suppe and Medwedeff, 1990) . These folds characteristically show steep to overturned beds within forward facing limbs (Suppe, 1985; Ramsay and Huber, 1987; Suppe and Medwedeff, 1990). Commonly, fault-propagation folds will become locked because some formations may form tight folds more readily than others. When folding ceases, the fault breaks through in a fracture mode; the fault may propagate along the

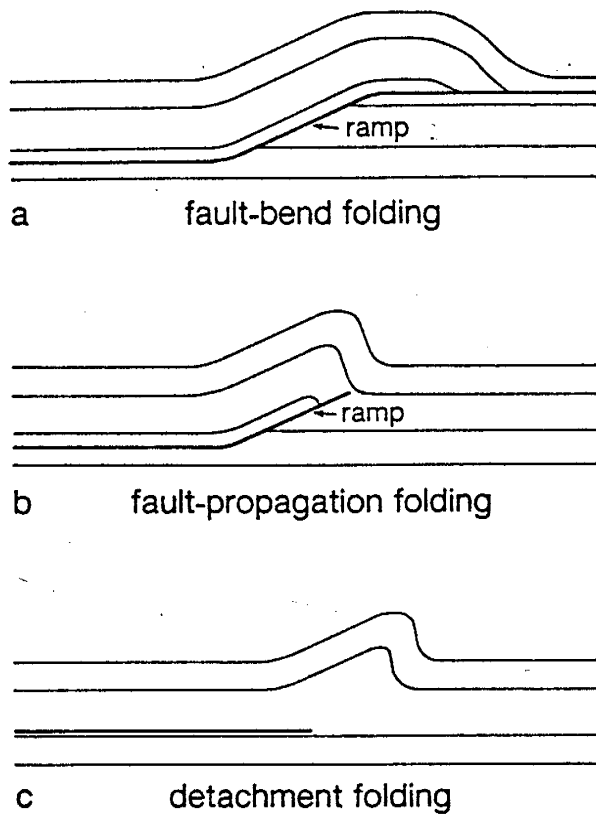


Figure 30. Three types of fold-thrust interactions: (a) a fault-bend fold, (b) a fault propagation fold, and (c) a detachment fold (after Jamison, 1987).

anticlinal or synclinal axial surface or somewhere within the steep limb (Suppe, 1985; Suppe and Medwedeff, 1990). Slip along the new fault segment produces a characteristic set of fault-propagation folds (Suppe and Medwedeff, 1990). A synclinal breakthrough produces the characteristic 'snakehead' anticline (Fig. 31a), whereas an anticlinal breakthrough produces "the common tight to overturned syncline in the footwall ..." (Fig. 31b); and a "breakthrough within the steep limb combines all these features". Quantities defined in figure 32a are: γ_i are fold axial angles, γ^* is the fold shape, β_i are angles between fault and bedding after slip along the fault. The theory also predicts the formation of a fault-bend syncline.

Because the theory uses a kink model of fold development (Suppe and Medwedeff, 1990), both folds are reconstructed to kink folds. The reconstruction involves the tracing of one horizon which is representative of the structure and is continuous. This marker horizon is then reconstructed to a fold with angular hinges and straight limbs using the kink method of cross section construction (Suppe, 1985; p. 63 - 64). The kink method is preferred over the Busk method because, in nature, these folds commonly have straight limbs and relatively small hinge zones (Faill, 1973) and models with curvilinear hinges yield virtually the same angular relationships (Jamison, 1987). The rest of the fold is reconstructed based on the geometry of the marker horizon.

Fold A. The reason for applying fault-propagation theory rather than fault-bend theory is that the beds in the footwall are folded. The nature of the folding suggests that it is not related to drag (compare with figures 12a and 12b, pp. 39 and 40) so this structure

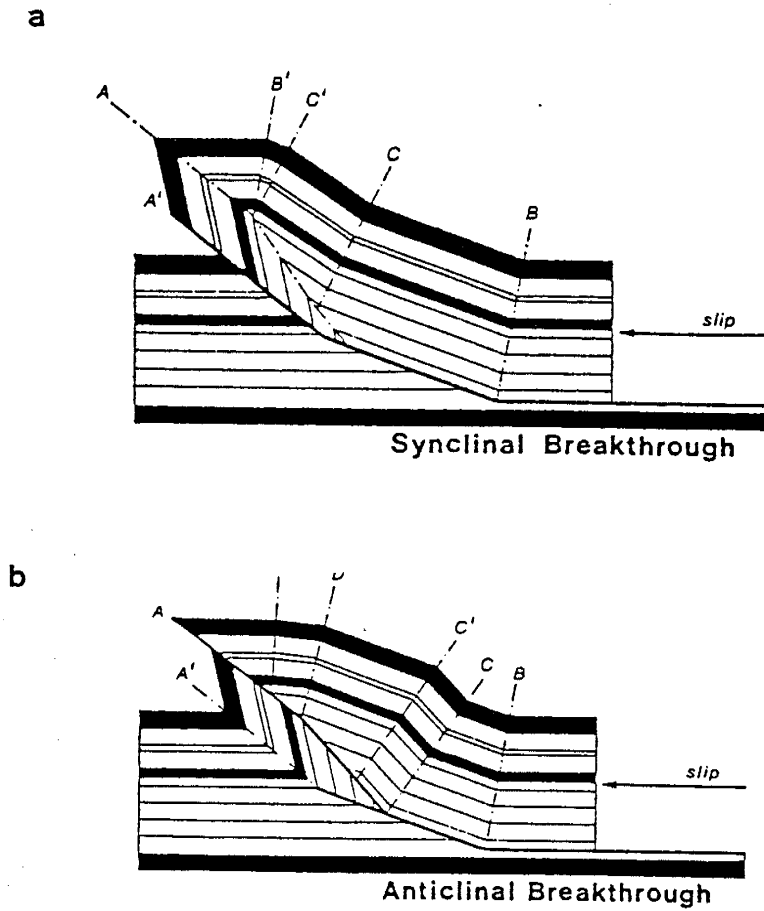


Figure 31. Balanced structural models showing (a) synclinal breakthrough structure and (b) anticlinal breakthrough structure (after Suppe and Medwedeff, 1990).

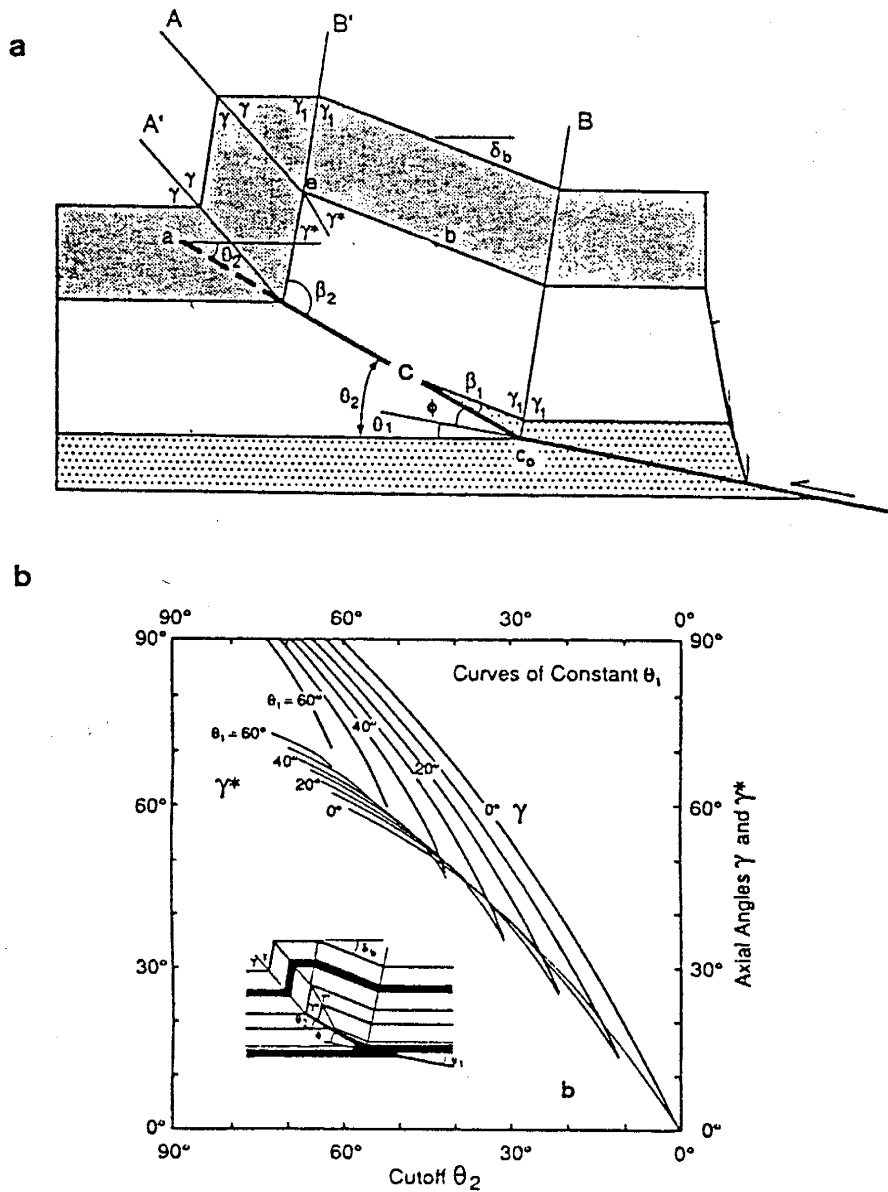


Figure 32. a) Schematic drawing of a general angular parallel fault-propagation fold. b) Relationship between fault shape, θ , and fold shape γ and γ^* for constant thickness fault-propagation folding with lines of constant cutoff angle θ_1 (after Suppe and Medwedeff, 1991).

is best treated as a fault-propagation fold with a steep limb breakthrough. Because of the complete exposure of both the fold and the thrust fault, a complete analysis is possible. A reconstructed sketch of the structure is shown in figure 33. Measurement of the axial angles gives: $\gamma = 66^\circ, 72^\circ$; $\gamma_1 = 79^\circ, 72^\circ$; and $\gamma_2 = 20^\circ, 14^\circ$. These angles have been averaged to give $\gamma = 69^\circ$, $\gamma_1 = 76^\circ$, and $\gamma_2 = 17^\circ$. The angle γ^* calculated from these values (eqn. 7; Suppe and Medwedeff, 1990) is 55° .

Two possibilities exist for why the forelimb is not steep or overturned, as is often the case (Suppe and Medwedeff, 1990). First, the fold could have locked before a tight structure could form producing the steep limb breakthrough. Second, the large interlimb angle could be the result of a low or negative differential bedding-parallel angular shear (Mosar and Suppe, 1992). At very low or negative angular shear the axial surface C (Fig. 32a) in the fold core dips at a steep angle. With increasing shear this axial plane has a shallower dip angle (Fig. 34). Comparison of figure 34 with figure 33 would suggest an angular shear of about -22.5° (Fig. 34d).

Fold B. Due to the steeply dipping forelimb the theory of fault-propagation can be applied. The fold is not as well exposed as Fold A, only the axial angle, γ , can be measured, however, the fold can be reconstructed using the fault-propagation theory. Measurement of the axial angle in figure 35a gives 45° . Assuming $\phi = 0$, the case for a simple ramp, then $\theta_1 = \theta_2 = \theta$. Using the graph in figure 32b, a value for θ in the range 0° to 30° can be obtained. A closer estimate of this angle can be obtained from the data in table 1 (p. 60). Averaging the ramp angles gives a value of 20° for θ . The

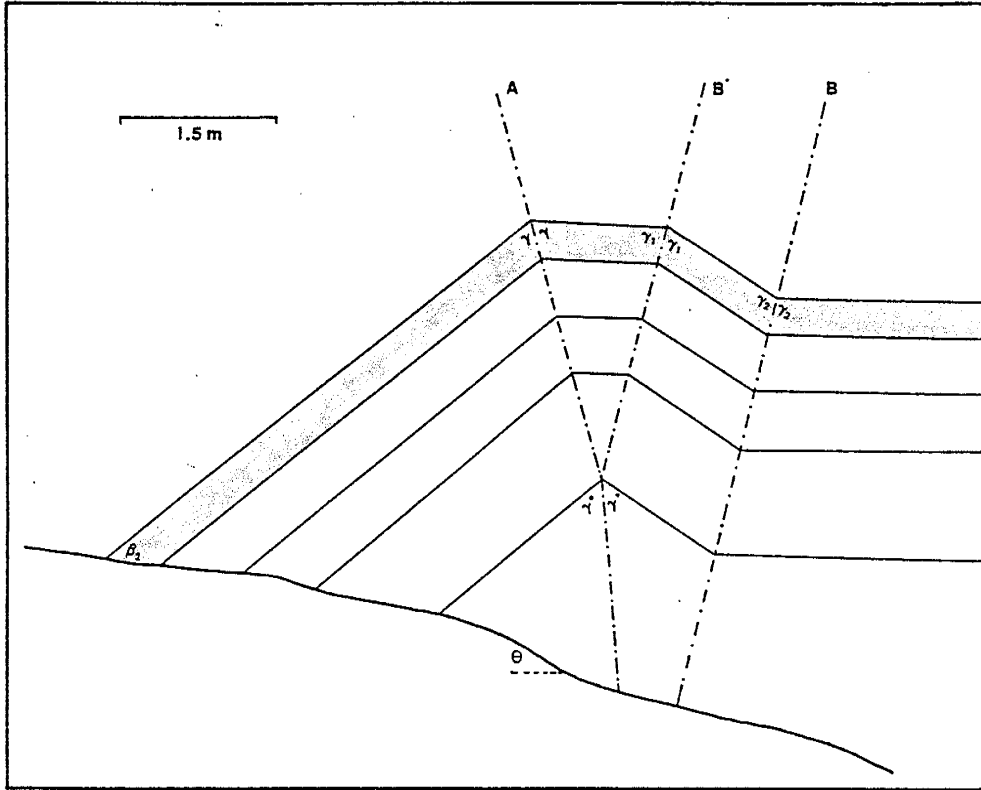


Figure 33. Sketch of fold in figure 8 using the kink method of reconstruction. The colored layer represents the bed that was traced from the photograph (marker horizon); the fold shape was reconstructed based on the marker horizon.

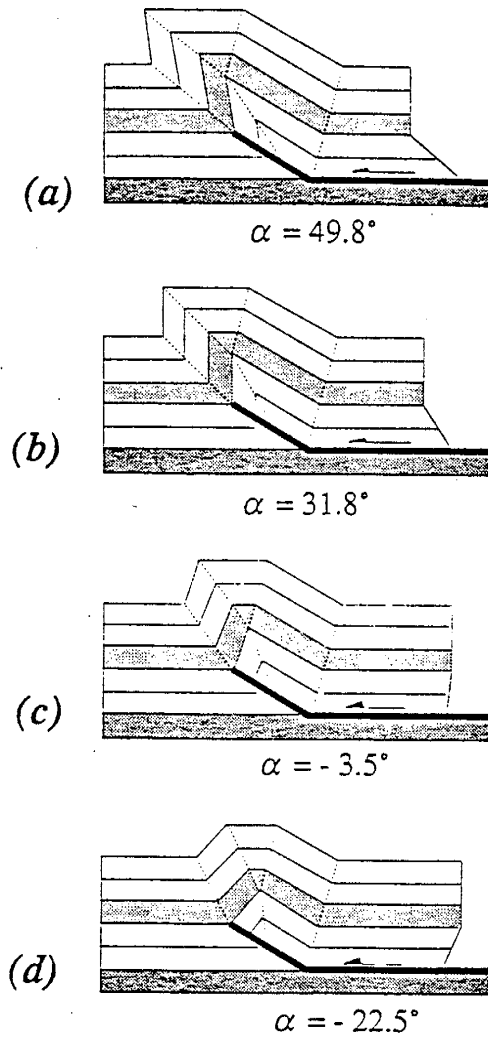


Figure 34. Influence of shear in fold core layers in simple-step fault-propagation folds with constant ramp height. Shear decreases from (a) through (d); step up angle for all four cases is 30° . Fold core angles, γ^* , are: (a) 25° , (b) 30° , (c) 40° , and (d) 50° (after Mosar and Suppe, 1992).

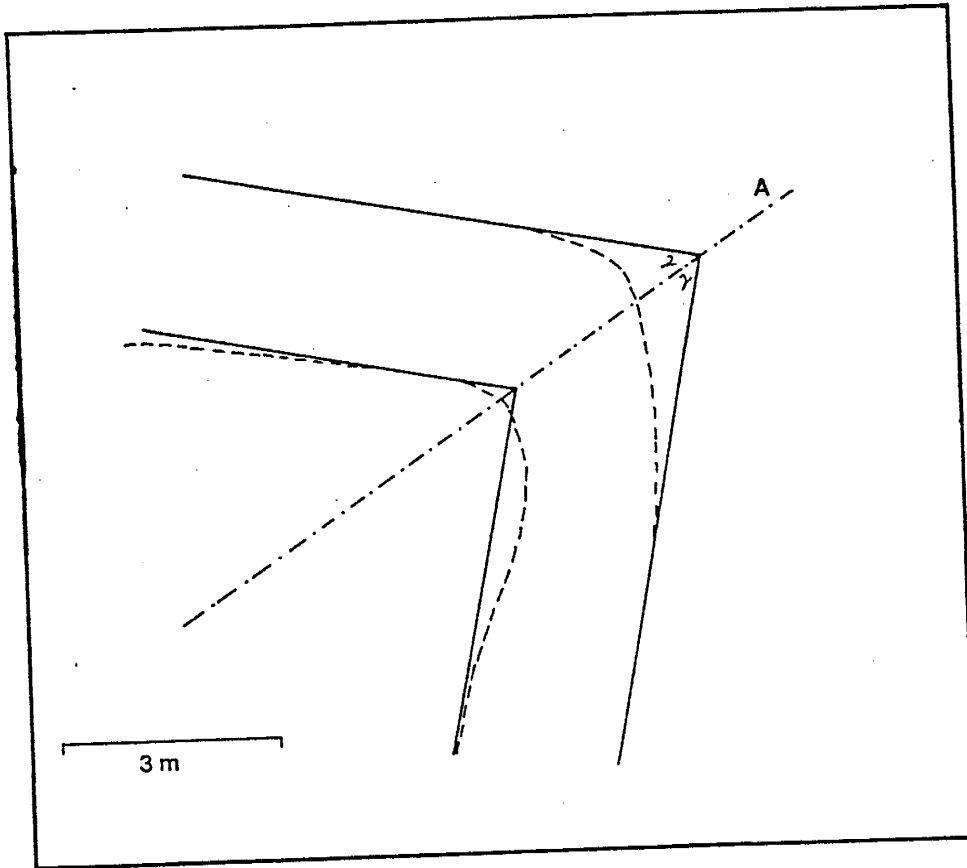


Figure 35a. Trace of marker horizon in figure 9 (dashed) and reconstructed using the kink method (solid).

dip of the backlimb is set equal to θ giving an axial angle, γ_1 , of 80° . The angle γ^* can be calculated (eqn. 7; Suppe and Medwedeff, 1990) as 35° . These data produce the shape depicted in figure 35b. Because the fault shape and location of the backlimb had to be estimated, a calculation of the depth to detachment is not possible. The synclinal structure associated with the anticline can be attributed to an adjacent ramp. This relationship is illustrated in figure 36.

Fold C. The relationship of this fold to the rest of the structure is not clear; it verges in the opposite direction. However, one possibility would be a drag fold in the footwall of a backthrust, the hangingwall and thrust surface of which have been eroded. Backthrusting is known to occur in this area; the backthrust in figure 11 (p. 38) strikes N40W and dips 10° NE.

Fold D. This structure could be related to drag by the hangingwall of the roof thrust (see Suppe, 1985; p. 342).

These folds could also have formed within a wrench zone. Kelly (1971) has documented the presence of localized intense deformation along wrench zones, such as the Y-O Buckle, in the Pecos Region. Chapin (1983) has interpreted the same type of deformation east of Socorro as resulting from movement along the Montoso-Paloma wrench faults. The deformation in the SW1/4, SW/14, Sec. 5 could also have resulted from similar conditions. However, in the SE1/4, SE1/4, Sec. 31, T.3 S., R.2 E. there is evidence for low-angle faults being offset by a northeast-striking fault. If this is the

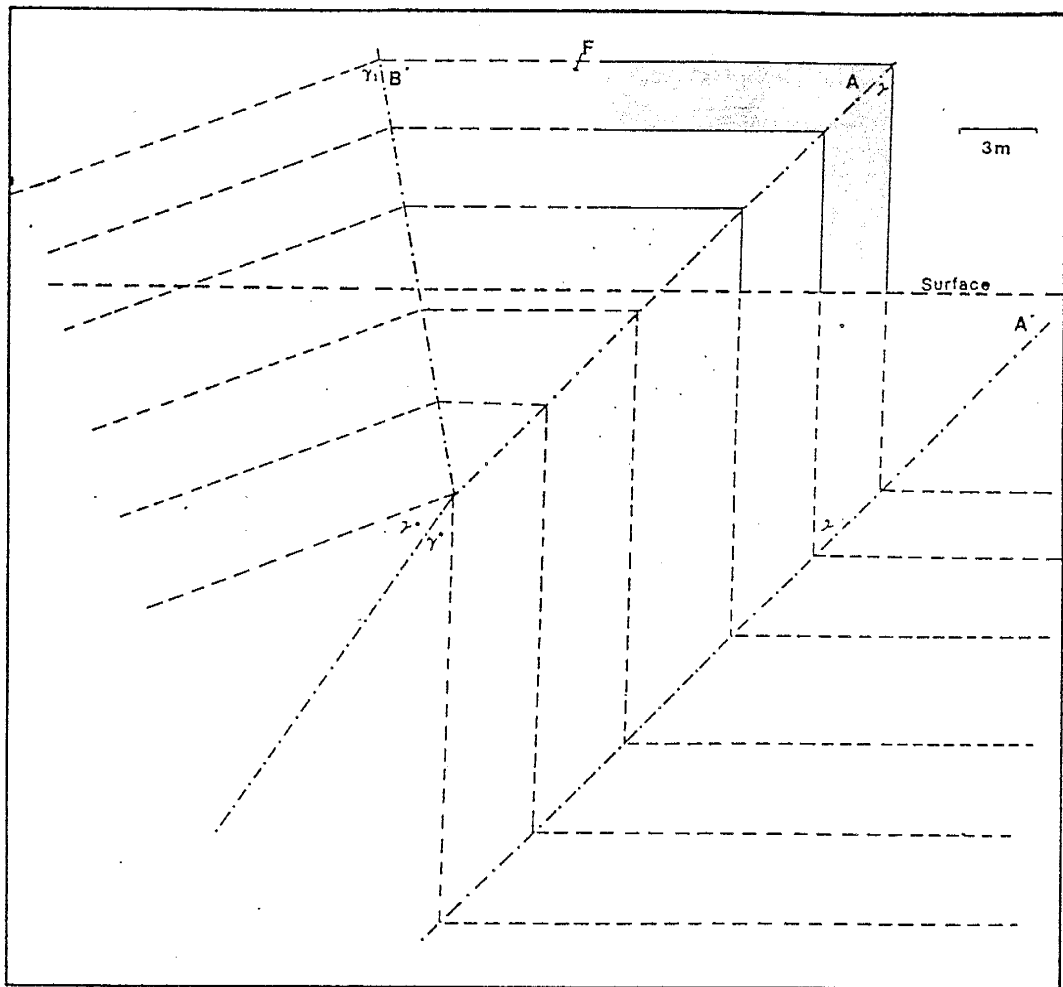


Figure 35b. Reconstructed fault-propagation fold based on data obtained from the marker horizon (colored) in figure 35a. Solid lines represent units exposed above the surface. Dashed lines represent what the beds would look like in subsurface and if Fault 7 did not offset the fold. F represents the approximate location of where Fault 7 will cut the fold.

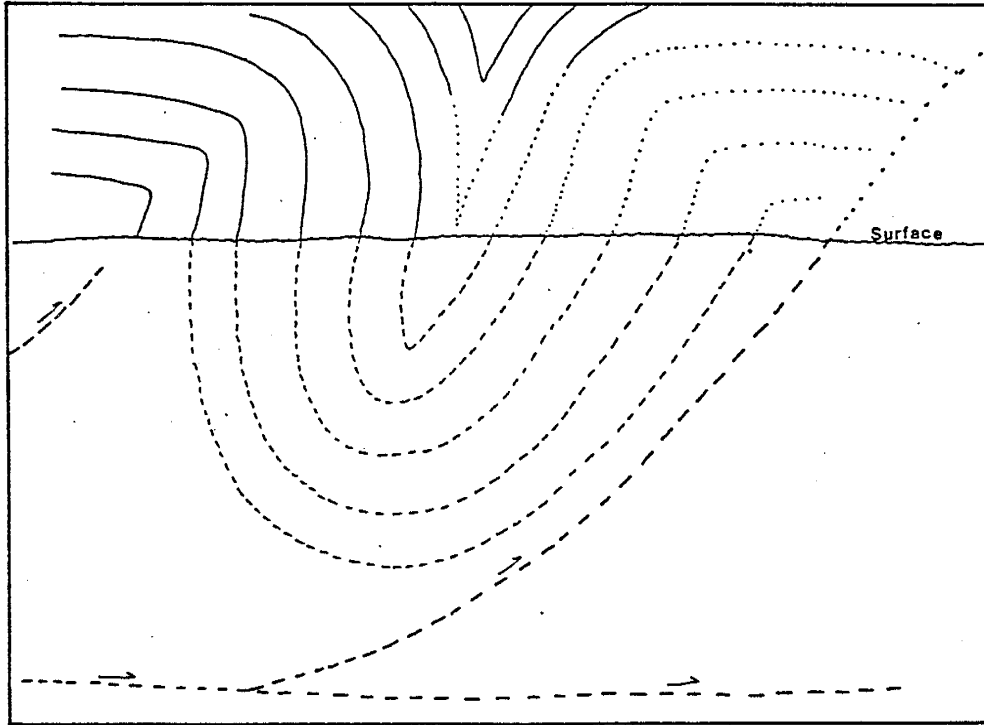


Figure 36. Possible interpretation of the tight fold in figure 9. Solid lines represent beds observed in outcrop. Dotted lines represent beds covered in outcrop. Dashed lines in subsurface represent structure in subsurface suggested by surface outcrops.

case, then the association of deformation in the SW1/4, SW1/4 Sec. 5 with wrenching becomes less attractive.

The north-south trending folds suggest an east-west orientation of the maximum principal stress. The orientation of Fold IV suggests a northwest-southeast shortening which may be related to Fault 7.

High-angle Fault Analysis

Fault 1. Due to the poor exposure of the fault surface it is difficult to determine whether it is high- or low-angle. At the one locality where the fault surface is exposed limestones of the San Andres Formation extend far enough into the arroyo to create a space problem for a low-angle fault (W. Beck, pers. com., 1992). Thus, a high-angle surface is preferred. The northwest limb of the syncline in this area is believed to have been steepened as a result of motion along the fault. This drag suggests a dip-slip component to the motion along the fault. The youngest strata offset by the fault is folded Santa Rosa Formation which constrains the faulting to post-date folding.

Fault 2. Exposure of fault surfaces are rare, the type of motion cannot be determined. The youngest strata offset by the fault is folded Meseta Blanca Member of the Yeso Formation. This constrains the age of the fault as post-north-south folding.

Fault 3. Kinematic indicators along the fault are rare, but stratigraphic offset suggests a dip-slip component to the motion. The fault only offsets strata of the Abo Formation.

Fault 4. Although Fault 4 is fairly well exposed, no kinematic indicators were observed. Stratigraphic offset suggests a dip-slip component to the motion. The youngest strata offset by the fault is the San Andres Formation. Movement on the fault occurred post-north-south folding.

Fault 5. Slickenside striae observed on some of the fault surfaces suggest a dip-slip component to the motion. The youngest strata offset by the fault is the lower Santa Fe Group. The fault is covered by the upper Santa Fe Group and Quaternary alluvium. The age of the fault is therefore constrained to the middle Tertiary.

Fault 6. Fault 6 is not well exposed, but drag folding in the Meseta Blanca and Torres Members of the Yeso Formation suggest a dip-slip component to the motion. The youngest strata offset by the fault is folded lower Torres Member of the Yeso Formation and is covered by the Glorieta and San Andres Formations. Motion along the fault is constrained to post-north-south folding, pre-reactivation of low-angle faults.

Fault 7. Striae can be observed in two locations: 1) where the fault offsets the steep limb of Fold IV, and 2) in the SW1/4, SW1/4, Sec. 5. At the first location striae suggest oblique motion. Striae observed at the second location suggest that a late component of motion on the fault plane was strike-slip; northeast side moved northwest relative to the southwest side (left-lateral). Left-lateral motion is also suggested by strike-separation. Drag folding in the Abo Formation suggests oblique, left-lateral

motion. The youngest stratum offset by Fault 7 is the middle Cretaceous Dakota Sandstone (Fagrelius, 1982) suggesting an upper Cretaceous age to faulting.

Contoured slickenside striae data from location 1 show three areas of concentration (Fig. 19b, p. 55). The first area of concentration is probably related to small thrust faults associated with the fold (see Fig. 15, p. 45). Slickensides which form the second area of concentration are predominantly bedding parallel (note relationship with the bedding plane great circle) and probably resulted from flexural-slip during folding. The third area of concentration is related to a low-angle surface which shows normal motion; the significance of this concentration is not known.

Fault 8. Fault 8 is not well exposed, but because it is a branch of Fault 7 it probably also had oblique-slip motion. It is probably the same age as Fault 7 as well.

Faults 9-13. Slickenside striae observed on some of the fault surfaces suggest a dip-slip component of motion. The faults offset folded Madera Formation through lower Meseta Blanca Member of the Yeso Formation. Fault motion occurred after north-south folding.

Fault 14-15. The fault surfaces are not well exposed, but stratigraphic offset suggests a dip-slip component to the motion. Offsets are confined to the eastern ridge.

Fault 16. Drag folding within the Torres Member of the Yeso Formation suggests that the motion was oblique-slip; drag folds within the Meseta Blanca Member of the Yeso

Formation on the downthrown side indicate dip-slip. The strike-slip component is right lateral and the dip-slip component is down-to-the-southwest. The youngest strata offset by Fault 16 are middle Permian in age. However, the orientation and type of motion suggest it is related to the same deformational event as Fault 7.

Origin of Faults

Northeast-striking Faults

Motion along the northeast-striking faults could not be determined and therefore will not be discussed.

Northwest-striking Faults

Northwest-striking faults confined to the eastern ridge (14 and 15) are most likely related to reactivation stress within the upper plate of the gravity slides rather than a regional stress system. As the block moved small adjustment breaks might have occurred.

The remaining northwest-striking faults could be related to a left-lateral wrench fault system with Fault 7 as the main wrench fault. Faults 8 and 6 could be synthetic and antithetic, respectively, to Fault 7. The dihedral angle between Fault 8 and 6 is 50° suggesting the two faults could be considered a conjugate fault systems. The angle between Fault 7 and 8 is 10° , and the angle between Fault 7 and 6 is 55° . Faults 9 - 13 could be tension fractures.

Movement along Fault 16 requires a principal stress orientation of N06E and

movement along Fault 7 requires a principal stress orientation of N74W (Wilcox, et. al, 1973).

North-striking Faults

Rejas (1965) first interpreted the north-striking faults as being genetically related to Rio Grande rift tectonism. Similar interpretations were made by Maulsby (1981) and Fagrelus (1982). Within the study area, only Fault 5 can be directly related to rift activity, it offsets the lower Santa Fe Group. Fault 4 could be related to rifting, a conjugate to Fault 7, or related to reactivation stress. Because it is confined to the ridge and is only known to offset the uppermost low-angle fault it is more likely related to reactivation stress. Fault 6 could also be related to rifting but it is more likely a conjugate of Fault 7.

Low-angle Fault Analysis

Older beds over younger

Orientation of the structure suggests a northeast-southwest shortening. Reverse motion is suggested by stratigraphic offset, drag folding, and rare slickenside striae. Restoration of this structure (Fig. 37) by line-length balancing techniques (Dahlstrom, 1969; Ramsay and Huber, 1987) gives a total shortening of 25%; 6% through faulting, 19% through folding. Because the arroyo cuts the structure at about 70° the error on this estimate is approximately 5%. This estimate is probably more realistic than Cabezas' (1991) estimate of 3%.

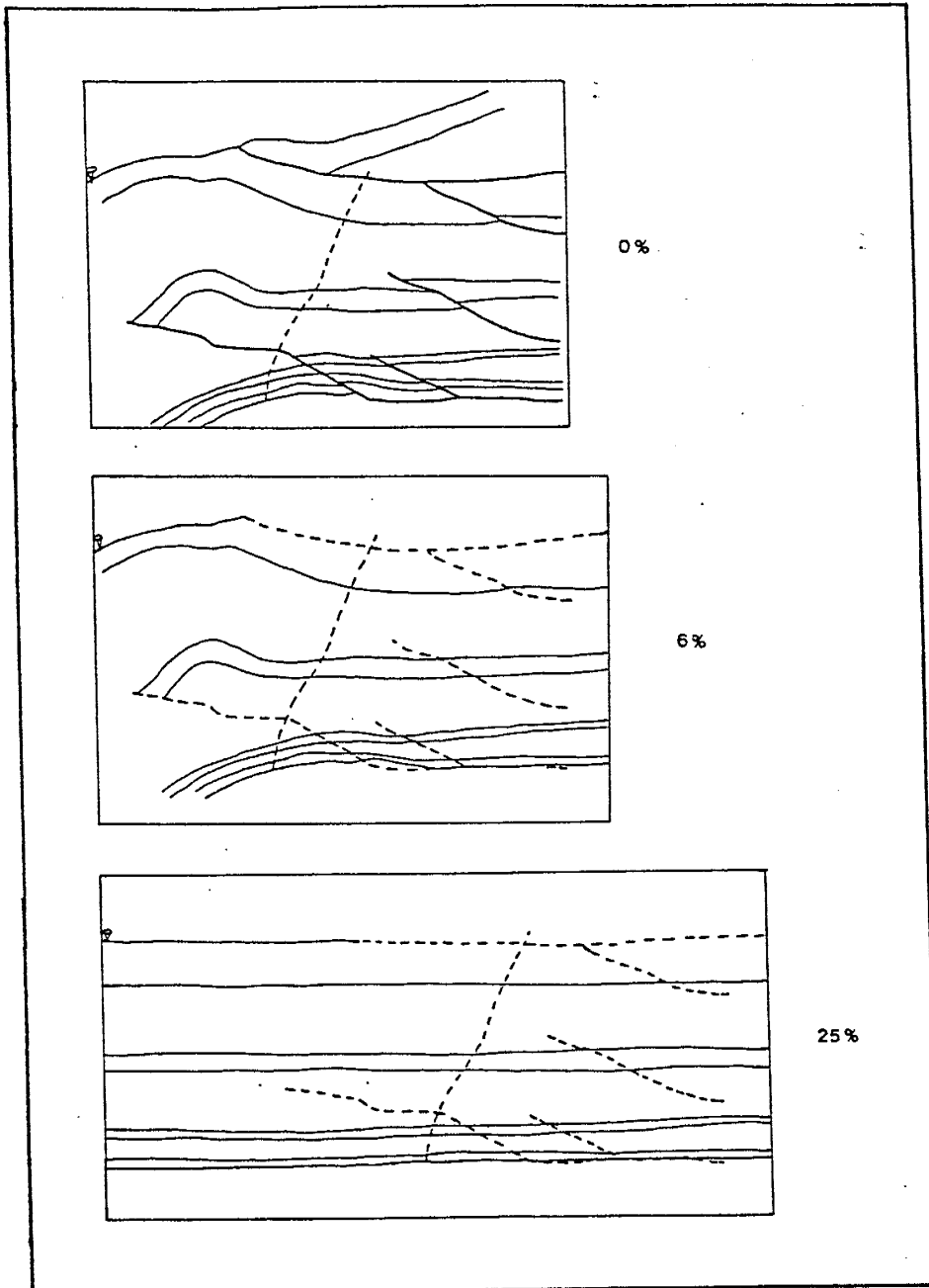


Figure 37. Restoration of duplex in figure 21 by line length balancing. Dashed lines represent locations of faults after restoration.

Younger beds over older

The type of motion on these faults cannot be determined accurately because not many directional indicators were found. One set of striae found on a small ramp within the San Andres Formation suggests reverse motion. Omission of strata and the younger over older relationship displayed by the faults suggest that they are detachments. Figure 38 shows that thrust faults can place younger beds over older beds.

Map and field relationships suggest two possible origins for these faults. First, they could be the youngest structures in the study area and originated as gravity slides. Second, the faults could be the oldest structures in the study area, possibly related to thrust faulting in the SW1/4, SW1/4, Sec. 5. and then reactivated. The key to discerning which of the two possibilities is more plausible lies in the folding in the area. If the allochthons are gravity slides associated with movement along high-angle faults, then they would not have been subjected to the folding the rest of the area has experienced. Although thrust and gravitational glide surfaces are rarely planar (Suppe, 1985), the magnitude and character of the folding should be different. Within the field area the allochthons and older strata show the same character and magnitude of folding, suggesting that both experienced the same event. Thus, it is proposed that these faults are the oldest structures in the study area and were reactivated by a different stress system than that which caused the low-angle faulting.

Geothermometry Analysis

The thickness of strata covering the study area during middle Tertiary was

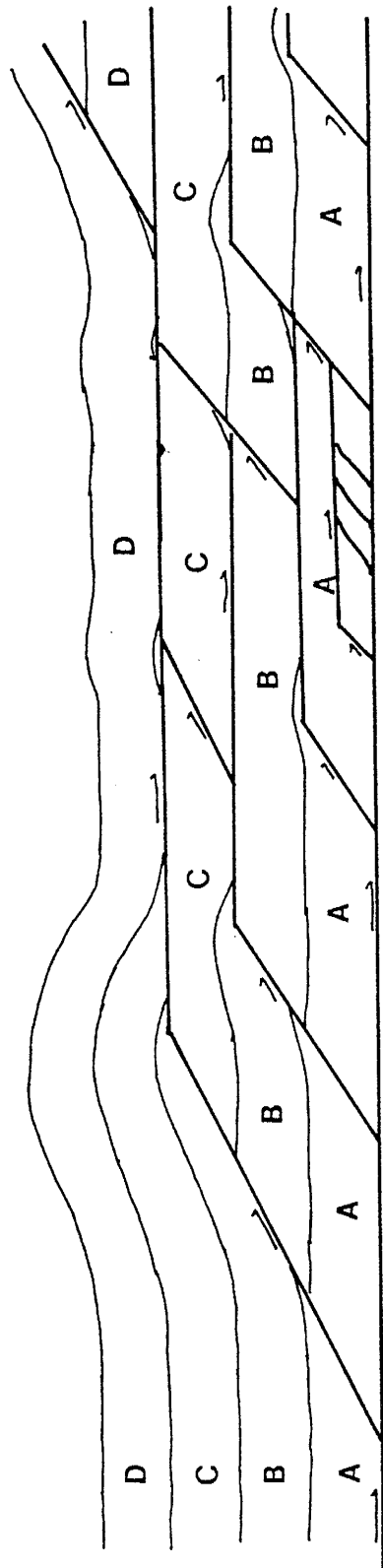


Figure 38. Schematic sketch of a thrust sheet demonstrating the placement of younger strata over older strata.

approximately 5 km (F.M. Craig, unpub. data). The present heat flow in the area is approximately 2.5 hfu. This heat flow would give an average geothermal gradient of 35 °C/km (M. Reiter, pers. com., 1992). Assuming the heat flow at maximum burial was about the same as it is now, burial temperatures for rocks now exposed at the surface would have been approximately 175 °C. The samples with silica crystallite temperatures of approximately 200 °C could be the result of fluids (groundwater) circulating through the rock. The low-angle and high-angle faulting would probably have produced adequate conduits for circulating groundwater. It is also possible that the geothermometry reflects a higher geothermal gradient.

Temperatures above 300 °C are too great to be explained by the above geothermal model. The wide range in temperatures obtained from those samples suggests there is a problem with the data. The most likely explanation for the high temperatures is that the samples are contaminated by detrital or vein quartz. Detrital and vein quartz do not grow from a gel; they are precipitated directly from solution. Quartz formed in this manner will have a large crystallite size regardless of temperature. The crystallite size measured from the diffractogram is a volume average of everything in the sample. If the sample contains enough vein or detrital quartz the results will be biased to a higher temperature. Chert examined in thin-section or oil will have a jigsaw puzzle texture because each grain is composed of smaller crystals, each oriented differently. Vein and detrital quartz examined in the same manner will not show this texture because they are single crystals. Analysis of the powdered samples in oil suggests the possibility of contamination by detrital quartz (J. Renault, pers. com., 1992).

STRUCTURAL HISTORY

The study area has been subjected to at least three deformational episodes (Table 2). The first episode resulted in the emplacement of the low-angle faults and folds. The second episode formed the northeast- and northwest-striking high-angle faults. The third episode was related to the development of the Rio Grande rift.

Table 2. Summary of deformation within the study area.

Episode	Structures	Max. Principal Stress Orientation
1	Low-angle faults Macroscopic folds	east-west
2	NE-striking faults NW-striking faults	N70W, N06E (?)
3	Rift faults Reactivation (?)	vertical

Episode 1

The orientation of both the low-angle faults and macroscopic folding suggest a maximum principal stress orientation of approximately east-west. The low-angle faulting and associated mesoscopic folds formed first, followed by, or occurring simultaneously with, the formation of the macroscopic folds. The age of this deformation can be constrained by determining the age of the folding. The age of the macroscopic folding is post-upper Triassic. The folds are offset by upper Cretaceous northwest-striking faults and by pre-upper Cretaceous northeast-striking faults. The best age constraint on this

deformation is post-upper Triassic and pre-northeast-striking faulting.

Episode 2

Stratigraphic offset suggests post-Triassic, pre-middle Cretaceous age for the northeast-striking faults. Northeast-striking faults also offset the macroscopic folds, the age is further constrained to post-middle Cretaceous, pre-northwest-striking faulting. In the Cerro del Viboro area, northeast-striking faults offset upper Cretaceous strata but are earlier than the northwest-striking faults (Fagrelus, 1982). Because the type of motion on the faults is not known, it is impossible to determine the orientation of the maximum principal stress.

The orientation of the maximum principal stress rotated from east-west to N70W, as determined from left-lateral motion on Fault 7, during the late Cretaceous. Fold IV and Faults 8 and 6 could have formed during the early stages of the deformation. The dihedral angle between Faults 7 and 8 is 10° and between Faults 7 and 6 is 55° . These angular relationships suggest that Fault 8 is synthetic to Fault 7 and Fault 6 could be antithetic to Fault 7 (Wilcox, et. al., 1973). Fold IV would have formed contemporaneously with Faults 8 and 6. For a true simple shear, the angle between the fold axis and the strike of the wrench zone is always less than 45° (Wilcox, et. al., 1973). The angle between the axis of Fold IV and the average orientation of Fault 7 is 55° . Several factors influence the shape and trend of folds, but only two are pertinent to this application. These are: 1) changes in the strike of the wrench fault; and 2) large components of vertical displacements (Wilcox, et. al., 1973). Fault 7 displays both of

these. In addition, this is probably not a case of true simple shear and the angle of 55° can be considered in the ballpark.

Continuing deformation leads to rotation of the conjugate faults away from an acute angle. In a left-lateral wrench system, this rotation is clockwise for synthetic faults and counterclockwise for antithetic faults. Formation of a throughgoing master wrench fault will add a net counterclockwise rotation to the deformation. Conjugate faults initially form at an angle of 60° to 70° (Wilcox, et. al., 1973). The angle of 50° between faults 8 and 6 probably implies only minor rotation.

In addition to conjugate faulting and en echelon folding, tension fractures form during the early stages of deformation (Wilcox, et. al., 1973). Tension fractures form parallel to the minor axis of the strain ellipse. For a left-lateral wrench system oriented N25W, the major axis of the strain ellipse will be oriented N20E and the minor axis will be oriented N70W. The present orientation of Faults 9 - 13 ranges from N60W to N70W. These faults, with minor rotation, could easily be tension fractures.

Development of a throughgoing master wrench fault occurs in the late stages of the deformation offsetting previously mentioned structures (Wilcox, et. al., 1973). Such is observed in the study area where Fault 7 offsets Faults 8 and 6 and Fold IV.

The orientation of Fault 16 suggests it is related to this deformational episode, however, right-lateral motion makes this correlation problematic. The timing of Fault 16 cannot be determined accurately based on available field evidence. The relationship with Fault 7 cannot be determined either. The only alternative is to shift the orientation of the maximum principal stress to N06E. This shift probably occurred during the same

deformational episode.

Episode 3

Rifting in the Socorro area began approximately 32 m.y., ago with rapid extension beginning about 29 m.y. ago (Chapin, 1989). Volcanism associated with the early stages of rifting consisted of sparse pyroclastic activity. Eruption of immense silicic ash-flow tuffs and basalts occurred in the interval 28.9 - 27.3 Ma (Chapin, 1989). Block-faulting was also initiated at this time and was characterized by domino-style faulting (Chamberlain, 1983). Late rift-faulting, which occurred between late Miocene and early Pliocene, is characterized by single faults or en echelon fault systems (Chamberlain, 1983; deVoogd, et. al., 1986). Fault 5 within the study area is a late rift, en echelon fault system.

The age for reactivation of the allochthons in the eastern part of the study area is constrained to post-northwest-striking faults. The possibility exists that reactivation was contemporaneous with northwest-striking faults. The acquisition of gravitational potential energy would result from vertical movement associated with Faults 7 and 16, i.e. slumping of the upthrown blocks to cover the faults. Slumping would have resulted in movement towards the east. This is also consistent with the allochthons being offset by a rift fault, if Fault 4 were considered as related to rifting. However, in order for reactivation to be mechanically possible and for Fault 7 to be covered, the motion would have to be towards the west with the allochthon sliding down the ramp. This suggests a post-northwest-striking fault reactivation age which is either pre-rift or

contemporaneous with rifting. Because rift faults are currently active (A.R. Sanford, pers. com., 1992), reactivation and motion along north-south faults could be occurring simultaneously.

Regional Implications

Chapin and Cather (1981) have proposed a two-stage Laramide orogeny for New Mexico. The first stage occurred from late Cretaceous to middle Paleocene and was related to an increase in the subduction rate of the Farallon Plate. Because of the shallow angle of subduction, the Farallon plate was viscously coupled to continental crust of the Colorado Plateau (Chapin and Cather, 1981). During this stage the maximum principal stress was oriented N70E. The second stage occurred from late Paleocene to early Eocene. The orientation of the maximum principal stress rotated to N45E in response to a counterclockwise rotation of the North American Plate during the opening of the Norwegian Sea (Chapin and Cather, 1981). Strain rates for the Laramide reached a maximum during the mid-Eocene (Cather and Johnson, 1984).

In the study area, Episode 1 deformation (low-angle faulting and macroscopic folds) could have formed during the early stages of the Laramide orogeny. If a component of motion on northeast-striking faults was right-lateral, these could have formed late in the early stage of the Laramide orogeny. Orientation of the Episode 2 maximum principal stress for northwest-striking faults does not agree with either of the orientations determined by Chapin and Cather (1981). This suggests that there could have been more than two stages of Laramide deformation. Bergh and Snoke (1992) have

demonstrated three distinct Laramide structural trends in the south-central Wyoming Foreland.

Beck and Chapin (1991) have documented northwest-striking wrench faults in the Joyita Hills, but it was possible to interpret these as antithetic faults to a larger north-striking wrench fault system with a principal stress orientation of N49E. This stress orientation agrees well with Chapin and Cather's (1981) estimation of N45E. Faults 6, 7, 8, and 16 could be considered as secondary faults of a larger wrench system. The master wrench fault would be oriented approximately N05W or N45E, depending on the type of conjugate. Right-lateral motion along a wrench fault striking N05W requires a maximum principal stress orientation of N41E. However, detailed mapping of the entire region will need to be completed before this hypothesis can be properly evaluated.

REFERENCES

- Altares, T., 1990, Stratigraphic description and paleoenvironments of the Bursum Formation, Socorro County, New Mexico [MS Thesis]: Socorro, New Mexico Institute of Mining and Technology, 189 pp.
- Baars, D. L., 1962, Permian System of Colorado Plateau: Amer. Assoc. Petrol. Geol., v. 46, p. 149 - 218.
- Bates, R. L., R. H. Wilpolt, A. J. MacAlpin and G. Vorbe, 1947, Geology of the Gran Quivira Quadrangle, New Mexico: New Mexico Bureau of Mines and Mineral Resources Bull. 26, 57 pp.
- Bauch, J. H. A., 1982, Geology of the central area of the Loma de las Cañas Quadrangle, Socorro County, New Mexico [MS Thesis]: Socorro, New Mexico Institute of Mining and Technology, 115 pp.
- Beck, W. C., 1991, Basement structures and influence of Phanerozoic deformation: Structural data from the Joyita Hills, Socorro County, New Mexico [abs.]: New Mexico Geological Society Proceedings Volume, p. 17.
- _____ and C. E. Chapin, 1991, Structural data from the Joyita uplift: implications for Ancestral Rocky Mountain deformation within central and southern New Mexico, in, Barker, J. M., B. S. Kues, G. S. Austin, and S. G. Lucas, eds., Geology of the Sierra Blanca, Sacramento, and Capitan Ranges: New Mexico Geological Society Guidebook 42, p. 183 - 190.
- _____, 1992, Oligocene-Miocene extension, detachment faulting and allochthonous terrain in the Joyita Hills, Central New Mexico [abs.]: New Mexico Geological Society Proceedings Volume, p. 15.
- Bergh, S. G. and A. W. Snoke, 1992, Polyphase Laramide deformation in the Shirley Mountains, south-central Wyoming Foreland: The Mountain Geologist, v. 29, p. 85 - 100.
- BLM, 1991, Quebradas: New Mexico Back Country Byway: U. S. Department of the Interior, Bureau of Land management brochure.
- Boyer, S. F. and D. Elliott, 1982, Thrust systems: Amer. Assoc. Petrol. Geol. Bull., v. 66, p. 1196 - 1230.
- Brown, K. B., 1987, Geology of the southern Cañoncito de las Uva area, Socorro County, New Mexico [MS Thesis]: Socorro, New Mexico Institute of Mining and Technology, 89 pp.

- Butler, R. W. H., 1982, The terminology of structures in thrust belts: *Jour. Struct. Geol.*, v. 4, p. 239 - 245.
- Cabezas, P., 1991, The southern Rocky Mountains in west-central New Mexico -- Laramide structures and their impact on the Rio Grande rift extension: *New Mexico Geology*, v. 13, p. 26 - 37.
- Cather, S. M. and B. D. Johnson, 1984, Eocene tectonics and depositional setting of west-central New Mexico and eastern Arizona: *New Mexico Bureau of Mines and Mineral Resources Circ.* 192, 33 pp.
- _____ and C. E. Chapin, 1989, Day 2: Field guide to upper Eocene and lower Oligocene volcanoclastic rocks of the northern Mogollon-Datil volcanic field, *in*, Chapin, C. E. and J. Zidik, eds., *Field excursions to volcanic terranes in the western United States, Volume 1: southern Rocky Mountain Region*: New Mexico Bureau of Mines and Mineral Resources Memoir 46, p. 60 - 68.
- Chamberlain, R. M., 1983, Cenozoic domino-style crustal extension in the Lemitar Mountains, New Mexico, *in*, Chapin, C. E., ed., *Socorro Region II: New Mexico Geological Society Guidebook 34*, p. 111 - 118.
- Chapin, C. E., 1978, Evolution of the Rio Grande rift - A summary, *in*, Riecker, R. E., ed., *Rio Grande rift: tectonics and magmatism*: Washington, D.C., American Geophysical Union, p. 1 - 5.
- _____, 1983, An overview of Laramide wrench faulting in the southern Rocky Mountains with emphasis on petroleum exploration, *in*, Lowell, J. D., ed., *Rocky Mountain foreland basins and uplifts*: Denver, Co., Rocky Mountain Association of Geologists, p. 169 - 179.
- _____, 1971, The Rio Grande rift, Part I: Modifications and additions: *New Mexico Geological Society Guidebook 22*, p. 191 - 201.
- _____, 1989, Volcanism along the Socorro accommodation zone, Rio Grande rift, New Mexico, *in*, Chapin, C. E. and J. Zidik, eds., *Field excursions to volcanic terranes in the western United States, Volume 1: southern rocky Mountains*: New Mexico Bureau of Mines and Mineral Resources Mem. 46, p. 46 - 57.
- _____ and S. M. Cather, 1981, Eocene tectonics and sedimentation in the Colorado Plateau - Rocky Mountain area, *in*, Dickinson, W. R and W. D. Payne, eds., *Relations of tectonics to ore deposits in the southern Cordillera*: Arizona Geological Society Digest v. 14, p. 173 - 198.
- Christiansen, P. W. and F. E. Kottowski, 1972, Mosaic of New Mexico's scenery, rocks, and history: *New Mexico Bureau of Mines and Mineral Resources Scenic Trips to The Geologic Past No. 8*, 170 pp.

- Colpitts, R. M., 1986, Geology of the Sierra de la Cruz area, Socorro County, New Mexico [MS Thesis]: Socorro, New Mexico Institute of Mining and Technology, 141 pp.
- Cordell, L., 1978, Regional geophysical setting of the Rio Grande rift: *Geol. Soc. Amer. Bull.*, v. 89, p. 1073 - 1090.
- Cullity, B. D., 1978, Elements of x-ray diffraction: Massachusetts, Addison-Wesely Publishing Co. Inc., p. 3 - 31, 81 - 148, 188 - 232.
- Dahlstrom, C. D. A., 1969, Balanced cross sections: *Canadian Jour. Earth Sci.*, v. 6, p. 743 - 757.
- deVoogd, B., L. D. Brown, and C. Merey, 1986, Nature of the eastern boundary of the Rio Grande rift from COCORP surveys in the Albuquerque Basin, New Mexico: *Jour. Geophy. Res.*, v. 91, p. 6305 - 6320.
- Darton, N. H., 1922, Geologic structure of parts of New Mexico: *U. S. Geological Survey Bull.* 726, p. 173 - 275.
- _____, 1928, "Red Beds" and associated formations in New Mexico: with an outline of the geology of the state: *U. S. Geological Survey Bull.* 794, p. 16 - 28
- Dunne, W. M. and D. A. Ferrill, 1988, Blind thrust systems: *Geology*, v. 16, p. 33 - 36.
- Elliott, D., 1976, The motion of thrust sheets: *Jour. Geophy. Res.*, v. 81, No. 5, p. 949 - 963.
- Fagrelus, K. H., 1982, Geology of the Cerro del Viboro area, Socorro County, New Mexico [MS Thesis]: Socorro, New Mexico Institute of Mining and Technology, 138 pp.
- Fail, R. T., 1973, Kink-band folding, Valley and Ridge Province, Pennsylvania: *Geol. Soc. Amer. Bull.*, v. 84, p. 1289 - 1314.
- Folk, R. L., 1974, Petrology of sedimentary rocks: Austin, Tx., Hemphil Publishing Co., 182 pp.
- Girty, G. H., 1909, The Manzano Group of the Rio Grande Valley, New Mexico: Part II, Paleontology of the Manzano Group: *U. S. Geological Survey Bull.* 389, p. 41 - 119.

- Gordon, C. H., 1907, Notes on the Pennsylvanian Formations in the Rio Grande Valley, New Mexico: *Jour. Geology*, v. 15, p. 805 - 816.
- Hawley, J. W., ed., 1978, Guidebook to the Rio Grande rift in New Mexico and Colorado: New Mexico Bureau of Mines and Mineral Resources Circ. 163, 241 pp.
- Hunt, A., 1983, Plant fossils and lithostratigraphy of the Abo Formation (Lower Permian) in the Socorro area and plant biostratigraphy of the Abo Red Beds in New Mexico, *in*, Chapin, C. E., ed., Socorro Region II: New Mexico Geological Society, Guidebook 34, p. 157 - 164.
- Kelly, V. C., 1971, Geology of the Pecos Country, southeastern New Mexico: New Mexico Bureau of Mines and Mineral Resources Memoir 24, 75 pp.
- _____, 1977, Geology of the Albuquerque Basin: New Mexico Bureau of Mines and Mineral Resources Memoir 33, 60 pp.
- Jamison, W. R., 1987, Geometric analysis of fold development in overthrust terranes: *Jour. Struct. Geology*, v. 9, p. 207 - 219.
- Jicha, H. L. and C. Lochman-Balk, 1958, Lexicon of New Mexico Geological names: Precambrian through Paleozoic: New Mexico Bureau of Mines and Mineral Resources Bull. 61, 137 pp.
- Keyes, C. R., 1903, Geologic sketches of New Mexico: Ores and Metals, v. 12, p. 48.
- _____, 1905, Geology and underground water conditions of the Jornada del Muerto, New Mexico: U. S. Geological Survey, water supply paper 123, p. 18 - 24.
- _____, 1906, Carboniferous Formations of New Mexico: *Jour. Geology*, v. 14, p. 147 - 154.
- King, R. E., 1945, Stratigraphy and oil-producing zones of the pre-San Andres Formations of southeastern New Mexico: New Mexico Bureau of Mines and Mineral Resources Bull. 23, 29 pp.
- Klug, H. P. and L. E. Alexander, 1974, X-ray diffraction procedures: New York, John Wiley and Sons, 966 pp.
- Kottlowski, F. E., 1963, Paleozoic and Mesozoic strata of southwestern and south-central New Mexico: New Mexico Bureau of Mines and Mineral Resources Bull. 79, p. 71.

- _____, R. H. Flower, M. L. Thompson and R. W. Foster, 1956, Stratigraphic studies of the San Andres Mountains, New Mexico: New Mexico Bureau of Mines and Mineral Resources Memoir 1, 132 pp.
- Lee, W. T., 1909, The Manzano Group of the Rio Grande Valley, New Mexico: Part I, Stratigraphy of the Manzano Group: U. S. Geological Survey Bull. 389, p. 5 - 40.
- Linden, R. M., 1990, Allochthonous Permian rocks in the Socorro region, central New Mexico: A structural analysis of emplacement and deformation [PhD dissertation]: Socorro, New Mexico Institute of Mining and Technology, 104 pp.
- Lucas, S. G., 1991a, Correlation of Triassic Strata of the Colorado Plateau and southern High Plains, New Mexico: New Mexico Bureau of Mines and Mineral Resources Bull. 137, p. 75 - 84.
- _____, 1991b, Triassic stratigraphy, paleontology and correlation, south-central New Mexico, *in*, Barker, J. M., B. S. Kues, G. S. Austin, and S. G. Lucas, eds., *Geology of the Sierra Blanca, Sacramento and Capitan Ranges, New Mexico*: New Mexico Geological Society Guidebook 42, p. 243 - 259.
- _____ and A. P. Hunt, 1989, Revised Triassic stratigraphy in the Tucumcari Basin, east-central New Mexico, *in*, Lucas, S. G. and A. P. Hunt, eds., *Dawn of the age of dinosaurs in the American Southwest*: New Mexico Museum of Natural History, p. 150 - 170.
- _____ and S. N. Hayden, 1989, Middle Triassic Moenkopi Formation, Nacimiento Mountains, north-central New Mexico, *in*, Lorenz, J. C and S. G. Lucas, eds., *Energy frontiers in the Rockies*: Albuquerque Geological Society, Rocky Mountain Section of the American Association of Petroleum Geologists, p. 16 - 17.
- _____ and O. J. Anderson, 1992, Triassic stratigraphy and correlation, west Texas and eastern New Mexico, *in*, Cromwell, D. W., M. T. Moussa, and L. J. Mazzullo, eds., *Transactions, Southwest Section, American Association of Petroleum Geologists*: SWS 92-90, p. 201 - 207.
- Maulsby, J., 1981, *Geology of the Rancho de Lopez area east of Socorro, New Mexico* [MS Thesis]: Socorro, New Mexico Institute of Mining and Technology, 85 pp.
- Mosar, J. and J. Suppe, 1992, Role of shear in fault-propagation folding, *in*, McClay, K. R., ed., *Thrust Tectonics*: London, Chapman and Hall, p. 123 - 132.

- Morley, C. K., 1986, A classification of thrust fronts: Amer. Assoc. Petrol. Geol. Bull., v. 70, p. 12 - 25.
- Needham, C. E. and R. L. Bates, 1943, Permian Type sections in central New Mexico: Geol. Soc. America Bull., v. 54, p. 1653 - 1668.
- Osburn, G. R. and C. Lochman-Balk, 1983, Stratigraphic nomenclature chart, *in*, Chapin, C. E., ed., Socorro Region II: New Mexico Geological Society Guidebook 34, p. 98.
- Ramsay, J. G., 1967, Folding and fracturing of rocks: New York, McGraw-Hill Book Co., 568 pp.
- _____ and M. I. Huber, 1987, The techniques of modern structural geology, V. 2: Folds and fractures: London, Academic Press, 400 pp.
- Renault, J., 1980, Application of crystallite size variation in cherts to petroleum exploration: New Mexico Institute of Mining and Technology, final report for grant No. 78-3315. 22 pp.
- Rejas, A., 1965, Geology of the Cerros de Amado area, Socorro County, New Mexico [MS Thesis]: Socorro, New Mexico Institute of Mining and Technology, 128 pp.
- Siemers, W. T., 1978, The stratigraphy, petrology, and paleoenvironments of the Pennsylvanian System of the Socorro region, west-central New Mexico [PhD dissertation]: Socorro, New Mexico Institute of Mining and Technology, 259 pp.
- _____, 1983, The Pennsylvanian System, Socorro region, New Mexico: Stratigraphy, Petrology, Depositional Environments, *in*, Chapin, C. E., ed., Socorro Region II: New Mexico Geological Society Guidebook 34, p. 147 - 155.
- Smith, C. T., 1983, Structural problems along the east side of the Socorro constriction, Rio Grande rift, *in*, Chapin, C. E., ed, Socorro Region II: New Mexico Geological Society Guidebook 34, p. 103 - 109.
- _____, G. R. Osburn, C. E. Chapin, J. W. Hawley, J. C. Osburn, O. J. Anderson, S. D. Rosen, T. L. Eggleston, and S. M. Cather, 1983, First day road log from Socorro to Mesa del Yeso, Joyita Hills, Johnson Hill, Cerros de Amado, Loma de las Cañas, Jornada del Muerto, Carthage, and return to Socorro, *in*, Chapin, C. E., ed., Socorro Region II: New Mexico Geological Society Guidebook 34, p. 1 - 28.

- _____, R. M. Colpitts and W. Gage, 1991, Structural geology of the Gonzales Precambrian Block, east of Socorro, New Mexico: a new look [abs.]: New Mexico Geological Society Proceedings Volume, p. 16.
- Starkey, J., 1970, A computer programme to prepare orientation diagrams, *in*, Paulitsch, P., ed., *Experimental and natural rock deformation*: Springer, p. 51 - 74.
- _____, 1977, The contouring of orientation data represented in spherical projection: *Can. Jour. Earth Science*, v. 14, p. 268 - 277.
- Stone, P. and C. H. Stevens, 1990, Triassic marine strata in east central California [abs.]: *GSA Abstracts with Programs*, v. 22, No. 3, p. 87.
- Suppe, J., 1983, Geometry and kinematics of fault-bend folding: *Amer. Jour. Science*, v., 283, p. 684 - 721.
- _____, 1985, *Principles of structural geology*: Englewood Cliffs, NJ, Prentice Hall, 537 pp.
- _____ and D. A. Medwedeff, 1990, Geometry and kinematics of fault-propagation folding: *Eclogae Geol. Helv.*, v. 83, p. 409 - 454.
- Thompson, M. L., 1942, *Pennsylvanian system of New Mexico*: New Mexico Bureau of Mines and Mineral Resources Bull. 17, 91 pp.
- Tosdal, R. M., 1990, Jurassic low-angle ductile shear zones, SE California and SW Arizona: thrust faults, extensional faults, or rotated high-angle faults [abs.]: *GSA Abstracts with Programs*, v. 22, No. 3, p. 89.
- Twiss, R. J. and E. M. Moores, 1992, *Structural Geology*: New York, W. H. Freeman and Company, p. 51 - 73, 217 - 261.
- Walker, J. D., M. W. Martin, J. M. Bartely and A. F. Glazner, 1990, Middle to Late Jurassic deformation belt through the Mojave desert, California [abs.]: *GSA Abstracts with Programs*, v. 22, No. 3, p. 87.
- Washington, P. A., 1987, *Mechanics of thrust fault formation* [PhD dissertation]: Storrs, The University of Connecticut, 203 pp.
- White, D., 1933, Some features of the early Permian flora of America: *International Geological Congress, Report of the XVI Session*, v. 1, p. 679 - 690.
- Wilcox, R. E., T. P. Harding, and D. R. Seely, 1973, Basic wrench tectonics: *Amer. Assoc. Petrol. Geol. Bull.*, v. 57, p. 74 - 96.

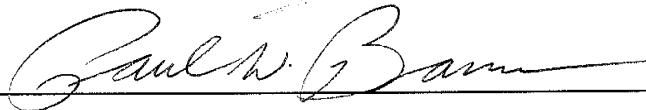
- Wilpolt, R. H., et. al., 1946, Geologic map and stratigraphic sections of Paleozoic rocks of Joyita Hills, Los Pinos Mountains and northern Chupadera Mesa, Valencia, Torrance and Socorro Counties, New Mexico: U. S. Geological Survey, Oil and Gas Investigations, Preliminary Map 61.
- _____ and A. A. Wanek, 1951, Geology of the region from Socorro and San Antonio east to Chupadera Mesa, Socorro County, New Mexico: U. S. Geological Survey Oil and Gas Investigations Map OM-121.
- Wood, G. H. and S. A. Northrop, 1946, Geology of the Nacimiento Mountains, San Pedro Mountains and adjacent plateaus of Sandoval and Rio Arriba Counties, New Mexico: U. S. Geological Survey, Oil and Gas Investigations, Preliminary Map 57.
- Yuras, W., 1976, The origin of the Lincoln Fold Belt, Lincoln County, New Mexico [MS Thesis]: Socorro, New Mexico Institute of Mining and Technology, 97 pp.

This thesis is accepted on behalf of the faculty
of the Institute by the following committee:



Adviser







Date